4707

POLYMER-LEATHER COMPOSITES V. PREPARATIVE METHODS, KINETICS, MORPHOLOGY, AND MECHANICAL PROPERTIES OF SELECTED ACRYLATE POLYMER-LEATHER COMPOSITE MATERIALS

Edmund F. Jordan, Jr., Bodhan Artymyshyn, Mary V. Hannigan, Robert J. Carroll, and Stephen H. Feairheller

Eastern Regional Research Center, Agricultural Research Service, U.S. Department of Agriculture
Philadelphia, Pennsylvania 19118

INTRODUCTION

This paper reviews an extensive study of largely reported work on polymer-leather composite materials (1-4). In this work two methods were utilized, for depositing selected acrylic polymers into the leather matrix by free radical polymerization (1). In one method polymer was introduced by emulsion polymerization into expanded hydrated panels. In the other, polymer was formed by bulk or solution polymerization in unexpanded acetone-dried panels. The widest feasible range of composite compositions was investigated for both methods. The kinetics of the emulsion process (2), together with the morphology (3) and mechanical properties (4) of both types of composites, were also investigated. In the present paper we attempt to combine the more important aspects of these detailed works into a comprehensive whole and to integrate this peripheral area of composite material science into the main body of work in the field.

It is well established today (5a-e) that the most industrially important composite materials containing polymer have only low concentrations (3-5%) of actual graft polymer. The core-shell model (5a) specifies that growth of the modifying polymer is restricted to discrete domains and fed by sorbed monomer; high grafting density is found only at the interfacial regions between domains, where, fortunately, it serves to insure interdomain adhesion, and thus greatly improve mechanical properties. In graft polymerization from emulsion, the polymer domains retain their initial colloidal size, but still possess core-shell

morphology. More intimate mixing can be achieved with anionic branched or block copolymers (5b), which have high graft density, or with free-radical initiated interpenetrating networks (5e), or their variants, where grafting is relatively infrequent. In the latter, domain sizes are often segmental (~100 A) but remain colloidal when prepared by emulsion polymerization. In all types of core-shell morphology, unextractable polymer results largely from being entrapped in cells surrounded by a matrix skin that is immiscible in the invading solvent. Consequently, this unretrievable polymer was formerly considered to be grafted.

With the matrix consisting of natural fibers of cotton, wool, or other types, an extensive literature (6-12) suggests that free-radical chemical grafting of the monomer to the fiber component, proceeding from primary radical attack to substrate, was the guiding mechanism affecting growth and morphology of the resulting composites. High energy radiation grafting (6,7) of cotton (13-20) and wool (9) probably induced high grafting incidence because the sole means of initiating chains by this technique depends on long-lived substrate radicals (post-irradiation grafting) or the relative G values for monomer and polymer (mutual grafting). High graft frequency is not necessarily inherent in chemical grafting, however.

Generally in chemical grafting of polymer to cotton and wool, a small quantity of fiber (1 g) was used with an excess of monomer (2 to 10 g) dispersed in a large quantity of water (or an aqueous non-solvent for the polymer) ~25-100 parts. The residual polymer in the fiber after solvent extraction was considered to be grafted and the extracted polymer used to estimate grafting efficiency (7,9,12). Saturation of fiber by polymer appeared to occur because graft yields were generally limited to 25 to 300%, even with excess monomer, and other forcing conditions (18-29). Thus an upper limit of fiber expansion (6,7,9,15-30) appears to restrict further deposition. This apparent saturation held both graft efficiency (13,17,27,30) and apparent graft frequency (13,15,18,29) to values much smaller than permitted by strict application of theory (8,9,11,13,18). Grafting by redox methods (20,21), by thermal decomposition of initiator (22), and other methods (7,9,11, 23-27), including use of oil soluble initiators (28,31) all gave similar, but limited, yield of graft polymer. Surprisingly, this same yield limitation appeared also to apply to the mechanistically favorable decomposition of Ce^{IV}-cellulose complex (32) to yield grafted composites with cotton (14,17-19). However, when the presence of popcorn polymer was suspected (9), yields reached the thousands (33,34) and even the millions (9). These results suggest that maintenance of the domain integrity of the modifying polymer within the fiber as polymerization proceeds (aided by free energy repulsions between substrate and polymer), to develop a morphology

analogous to the core-shell model (5a,c), is a viable alternate mechanism to grafting. Restriction of the deposition to a composition gradient extending throughout the microfibrillar and higher aggregation levels (3), accompanied by only interfacial grafting, would provide such a model. Polymer deposition should then be limited in volume by restraints imposed in maintaining most features of the original fiber, while allowing some limited lateral expansion. Tortuosity restrictions (5d) and interchain entanglements would limit the amount of homopolymer that could be extracted (12,35). Because precipitation polymerization (36a) results from the methods used to prepare all of these composites, the accompanying gel effect nearly always produced high molecular weight branches (6,7,9,12,15,18,29,30). Finally, preferential location of the available polymer within the fiber could only result from irreversible adsorption of initiator. This tendency is well documented (2,9,14,20,21,37). However, in spite of the intensive effort outlined above, the actual mechanism, or mechanisms, for producing bound polymer in fibers remains elusive (9,12).

A similar mechanism of deposition of polymer formed in situ in leather might be expected because the aggregation levels of cotton, wool, and leather are similar (1,3). Levels in leather proceed from nearly visible fiber bundles, 15 to 200 μm in diameter, composed of fibers, 1.5 to 5 μm in diameter, with the main structural elements crystalline fibrils, 650-2000 Å in diameter. These are subdivided further into protofibrils 35 Å, and, finally, into triple helical tropocollagen chains, 15 Å in diameter and 3000 Å long. The obvious difference between leather and other natural fibers (12) resides in the three dimensional fabric-like structure of leather. The matrix consists of densely packed fine fibers, with generally parallel conformation in the grain or surface region, yielding to coarser appearing, looser, diagonally interwoven aggregates of fibers (fiber bundles) in the corium region below.

In this paper, three acrylate monomers, namely methyl methacrylate (MMA), a mixture of n-butyl acrylate and methyl methacrylate (BA + MMA) containing 0.591 weight fraction of n-butyl acrylate and pure n-butyl acrylate (BA) were polymerized into chrome-tanned 5 oz cattlehide by a convenient emulsion process developed at this center (38-40), and a new method involving bulk or solution polymerization (1). In both processes the effect of composition on deposition yields, efficiencies, and apparent graft frequencies, as well as composite densities is emphasized in this work. The kinetics of the emulsion process is presented to shed light on the deposition mechanism. Photomicrographs of selected samples of the composites and of negative replicas prepared by preferential etching of the collagen fibers with dilute hydrochloric acid illustrate the morphology. Water absorption is used to monitor

the shielding effect of polymer on the matrix. Finally, mechanical properties are presented for all of the accumulated composite materials. An additional purpose of this presentation is to demonstrate certain similarities of the properties of these systems with the corresponding properties of commercially important synthetic composite materials, which have been extensively investigated (5a-b).

EXPERIMENTAL

Detailed Description

Detailed descriptions of all experimental procedures were presented in Parts I (1), II (2), III (3), and IV (4). Consequently, only brief outlines of experimental procedures and definitions are presented here to better enable the reader to follow this work.

Polymerization Procedure

Panels (8.9 x 15.2 x 0.235 cm) were cut consecutively, at all possible locations, from commercial chrome-tanned grain-split blue stock cattlehide. Untreated control panels were included with each treated panel. In the emulsion method, after a separate 30 min conditioning period with the potassium persulfate-sodium bisulfite redox initiator system, the panels to be treated were tumbled at ambient temperature under emulsion conditions with the appropriate monomer for 24 hr. Composite composition was obtained gravimetrically from methanol or air-dried panels. Homopolymer was removed from apparent bound polymer by hot benzene extraction. Standard conditions were: water 5:1 based on dry leather; $K_2S_2O_8$, 4 mole %, based on monomer; $NaHSO_3$/ $K_2S_2O_8$, 0.5; Triton X 100 (1.03%) 2 cc/g based on wet leather. For kinetic studies, the conditioning period was omitted, and smaller panels (~0.2 X) were used. Variable changes were made with the standard conditions used as points of departure. In the bulk or solution process, panels were saturated with pure monomers or monomers diluted with benzene, and the polymer present was polymerized with bis azoisobutyronitrile (AIBN) as initiator in sealed systems at 60°C.

Morphological, Physical, and Mechanical Properties

Real densities were determined by use of a helium-air pycnometer (1) and apparent densities by measurement of panel volumes (1). Neat polymer densities, in g cc^{-1}, were: MMA, 1.146; BA + MMA, 1.103; BA, 1.072, respectively. Light microscopy of stained sections was used to determine the thickness of layers of deposited polymer at grain and corium surfaces (discussed below). Rough

estimates of diffusion constants were obtained by monitoring the weight increase produced by monomer absorbed as a function of time into films of BA + MMA copolymer under approximate standard conditions. Light and scanning electron microscopies (SEM) were used to obtain photomicrographs (3) of thin sections and surfaces of the controls, composites, and their inverted replicas. The latter (called simply replicas in this work) were obtained by hot dilute hydrochloric acid digestion of the collageneous material from MMA composites, leaving a replication of the fibrous detail in the continuous polymer phase. Water uptake by total immersion of the composites and controls in water was followed as a function of time to 8 days at ambient temperature to obtain rate and equilibrium water absorptivities. Standard ASTM procedures were used for the mechanical properties and a Williamson* apparatus (4) was used for mechanical spectroscopy. Molecular weights were obtained with a Mecrolab 501 membrane osmometer.

Definitions

In this work, mole fraction is designated m; weight fraction, w; and volume fraction, ϕ. Subscripts are: 1, leather; 2, polymer; d, deposited polymer; b, bound polymer; max, maximum; a, apparent; r, real; p, synthetic polymer (or copolymer); f, float; t, total; l, layered. Quantities W and V represent specimen weight in g and volume in cc, respectively. Polymers deposited in leather are identified by their monomers, MMA, BA + MMA, BA, respectively. Other definitions are as follows:

$$\text{Fraction deposited} = W_2/W_1;\ \text{fraction bound} = W_{2b}/W_1 \qquad (1;1a)$$

Deposited, ε_d, and bound, ε_b, polymer efficiency fraction (1)

$$\varepsilon_d = W_d/W_T;\ \varepsilon_b = W_b/W_T \qquad (2;2a)$$

Bound polymer frequency fraction (1,18)

$$F_b = (\bar{M}_n\ \text{collagen}/w_1)/(\bar{M}_{n2}/w_b) = w_b\bar{M}_n\ \text{collagen}/w_1\bar{M}_{n2} \qquad (3)$$

W_T is the total weight of polymer obtained. The molecular weight of collagen was taken as 300,000 (1). Because % conversion-time curves for polymer deposition in the matrix was linear to nearly 100% conversion for all systems (2), a pseudo-zero order kinetic expression, equivalent to the fraction of monomer polymerized per unit time, is used in this work to express the initial rates of

*Reference to brand or firm name does not constitute endorsement by the U.S. Department of Agriculture over others of a similar nature not mentioned.

monomer [M] disappearance at locations in matrix and float. The expression is (2)

$$[M]_o - [M] = R_i t \qquad (4)$$

where R_i is in moles $l.^{-1}$ sec^{-1}. An IBM 1130 computer was used for curve fitting.

RESULTS AND DISCUSSION

A. Process Efficiencies and Composite Densities

In Table 1 are listed data for BA + MMA composite compositions, densities, number-average molecular weights, and graft frequencies. These were prepared under standard conditions in emulsion and by the bulk (or solution) polymerization techniques. They can be considered to be representative of the other two systems (MMA, BA) (1). The effect of time for an emulsion polymerization having a feed weight fraction of 0.5 is also included (section C). The rate of change of density with increase in the weight fraction of polymer, w_2, for the emulsion systems is considerably less than the corresponding rate by the bulk-solution method, reflecting the ability of the more expanded matrix of the former to accept polymer, yet retain more free space. The molecular weights for the emulsion systems, which generally decreased in the order: bound > deposited > float for each composition increment, illustrate a strong gel effect when compared with the molecular weight for the copolymer prepared in the absence of leather (experiment 7). Considerable microgel (20-50%) was also found in all of the isolated bound polymer, which, of course, contributed to their inability to be extracted by benzene before acid treatment. This provides clear evidence for polymer to polymer grafting. However graft frequencies, F_b, last column, were low, in harmony with results obtained for many other natural fibrous composites (7,9,13,15,18,29). It is also of interest that $\bar{M}_n$ was generally constant with time, for polymerization occurring in both matrix and float locations (section C).

Under standard conditions for polymerizations taken to 100% conversions (Fig. 1), a constant, designated D_e, representing the efficiency of deposition for the monomer systems employed (because $D_e = w_2/w_{2\ feed}$), varied as MMA > BA + MMA > BA. A similar order, Fig. 2, insert A, was found for the rate of polymer deposited, eq. (1). The reason for these orders can be seen in Figure 2 inserts B, C, D. These inserts show % conversion-time curves for polymer deposition in matrix and float, as well as the rate of bound polymer formation under standard conditions. Generally, bound polymer rate was about one half of that deposited in all three

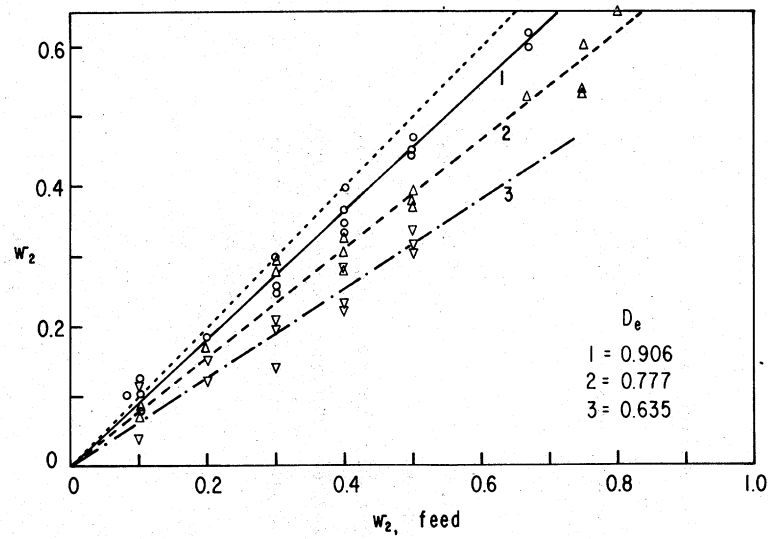

Fig. 1. The weight fraction of polymer deposited, w_2, versus the weight fraction of monomer in the feed, $w_{2\,feed}$. Designations are: curve 1, MMA; curve 2, BA + MMA; curve 3, BA. The slopes represent the deposition efficiency, D_e as given in the figure. The dotted line is $D_{e\,max} = 1.0$.

systems. In addition, the linearity of the deposition rate, which persisted to high conversions, suggests diffusion control of polymer growth in the matrix. For MMA, insert B, preferential deposition in the matrix, with little polymer formation in the float, was found at all conversions. In addition, the rate of deposition greatly exceeded the rate in the absence of leather. For BA + MMA, insert C, and BA, insert D, polymer initially formed in the leather, but polymerization activity was transferred to the float at an intermediate time before polymerization was complete. This behavior accounts for the trends in D_e, Figure 1. In contrast to MMA, the rate in the presence and absence of leather for BA + MMA insert C was nearly the same, while for BA the overall polymerization rate, R_T, was retarded by leather presence till a critical time, when a strong Tromsdorff (36a) acceleration was noted in the float. At long times, Fig. 3, insert A, and under forcing conditions (multiple exposure to fresh monomer under standard conditions) (1) the rate of deposition was slowed (dashed line) compared to the initial rates (solid lines) that persisted through several days of reaction. However, the efficiency of deposition was greatly reduced because most polymer formed in the float. In

Table 1. Compositions, Densities, and Molecular Weights of a Selection of BA + MMA - Leather Composites Prepared by Both Methods[a]

Expt. no.	w_2 feed	Composite composition w_2 deposited	Composite composition w_2 bound	Bound pol. frn.[b] W_b/W_d	Density g cc^{-1} deposited	Density g cc^{-1} bound	Molecular weights $\bar{M}_n$[c] bound	Molecular weights $\bar{M}_n$[d] deposited	Molecular weights $\bar{M}_n$ float	F_b
				A. Emulsion Polymerization						
1	0.103	0.0742	0.0338	0.437	0.622	0.618				
2	0.200	0.182	0.140	0.735	0.665	0.609	492,400		312,400	0.0993
3	0.301	0.294	0.260	0.838	0.601	0.572	605,300		606,000	0.174
4	0.401	0.327	0.279	0.795	0.614	0.573	592,900	891,200	242,400	0.195
5	0.500	0.372	0.306	0.746	0.712	0.616	1,263,200	918,200	505,000	0.105
6	0.750	0.528	0.353	0.488	0.812	0.605	1,162,000	365,100	140,950	0.141
7	1.0	1.0							168,350	
				B. Bulk or Solution Polymerization						
8	0.172	0.084			0.683					
9	0.250	0.195			0.807					
10	0.315	0.263			0.845					
11	0.306	0.310			0.962				88,300	
12	0.455	0.442			1.011			190,200		

13	0.479	0.467			1.107				132,050	
14	0.521	0.667			1.107					
					C. Emulsion Polymerization, Rate Study[e]					
	time, min									
15	30	0.0618	0.0383	0.605	0.609	0.624				0.0339
16	60	0.104	0.0775	0.720	0.590	0.623	744,300			0.0445
17	90	0.149	0.116	0.746	0.646	0.617	883,800			0.134
18	120	0.228	0.201	0.837		0.598	565,600	522,400		0.136
19	150	0.221	0.177	0.756	0.651	0.608	471,400	606,000		0.106
20	180	0.299	0.232	0.705	0.711	0.564	883,800	739,000		0.141
21	240	0.320	0.232	0.642	0.686	0.606	642,800	522,400	300,000	0.290
22	300	0.408	0.317	0.717	0.718	0.570	479,300	473,400	303,000	

[a] Similar data for MMA and BA systems may be found in reference 1, Tables I and V.

[b] Weight of bound polymer divided by the weight of that deposited.

[c] Insoluble in benzene; isolated by HCl etching of collageneous material.

[d] Fraction soluble in benzene.

[e] Another set of data, reference 1, plotted in Figure 2, insert C.

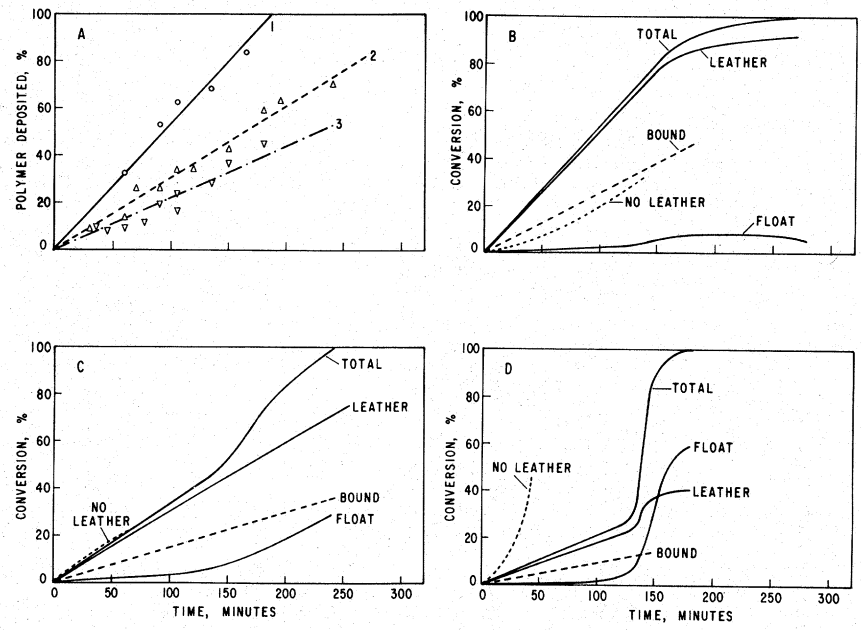

Fig. 2. Rate curves for total polymerization including composite formation with $w_{2\,feed} = 0.5$. Insert A, % polymer deposited in leather versus time; curve 1, MMA; curve 2, BA + MMA; curve 3, BA. Inserts B, C, D, percent conversion-time curves for: insert B, MMA; insert C, BA + MMA; insert D, BA. Concentrations were, in moles l^{-1}: MMA, $[M]_o = 1.84$, $[I] = 0.0741$; BA + MMA, $[M]_o = 1.62$, $[I] = 0.0643$; BA, $[M]_o = 1.44$, $[I] = 0.0585$; all based on water content.

fact, the constant for the efficiency of deposition based on the total polymer produced ε_d (Fig. 3, insert B) eq. (2) and the corresponding constant for bound polymer formation ε_b (insert D), eq. (2a) declined roughly monotonically with feed weight fraction and time, insert C. The system efficiency corresponding to D_e of Figure 1 was still in the order MMA > BA + MMA > BA. The data in these figures show that only a limited amount of polymer could be efficiently deposited in the leather matrix. This saturation amount was a function of the monomer used and declined with increase in the molar volume of the monomer. Under forcing conditions more polymer could be deposited, but only with greatly reduced efficiency. The effect of the polymer deposited in the residual free space in the matrix is treated next by considering composite densities.

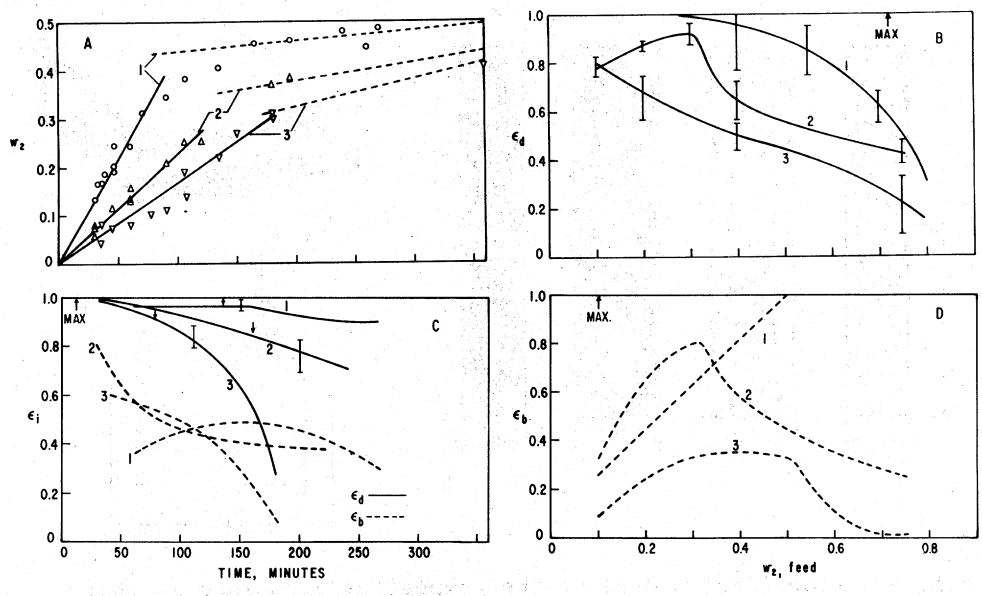

Fig. 3. Insert A, rates of formation of w_2 for recipe conditions with $w_{2\ feed} = 0.5$. Insert B, specific deposition efficiency, ε_d, as a function of $w_{2\ feed}$. Insert D is the same but with ε_b. Insert C compares ε_d, solid lines, and ε_b, dashed lines, as functions of time. Numbers in the figure correspond to 1, MMA; 2, BA + MMA; 3, BA. The maximum efficiency curve is indicated.

In the emulsion prepared composites, most of the polymer was observed (3) to deposit in untreated leather (shown schematically in Fig. 4, insert a) in the space around individual fibers, largely within the confines of fiber bundles (insert f). In this way, experimental panels or even full sheepskins (38) increased in thickness (insert b) without much change in area. The coarse polymer domains so formed (2 to 50 μm) were in marked contrast to the appearance of polymer depositing within the individual fibers of cotton (7,14) and wool (9), by a variety of polymerization techniques (1,3,7,9,14). In these systems domains as small as 20 A (9) but usually 0.1 to 3 μm (3,14) were routinely observed by transmission electron microscopy (TEM). Removal of soluble polymer by benzene extraction from the cattlehide composites (insert c) reduced the density (Table 1) while retaining the expanded volumes (1). A special feature of emulsion polymer deposition in cattlehide (not found for sheepskins or other thinner, looser leathers) (38,40) is shown in insert e, where the polymer deposited only in layers near the outer surfaces (comprising 25 to 60% of the cross section) (1), leaving the center section polymer free. A thin,

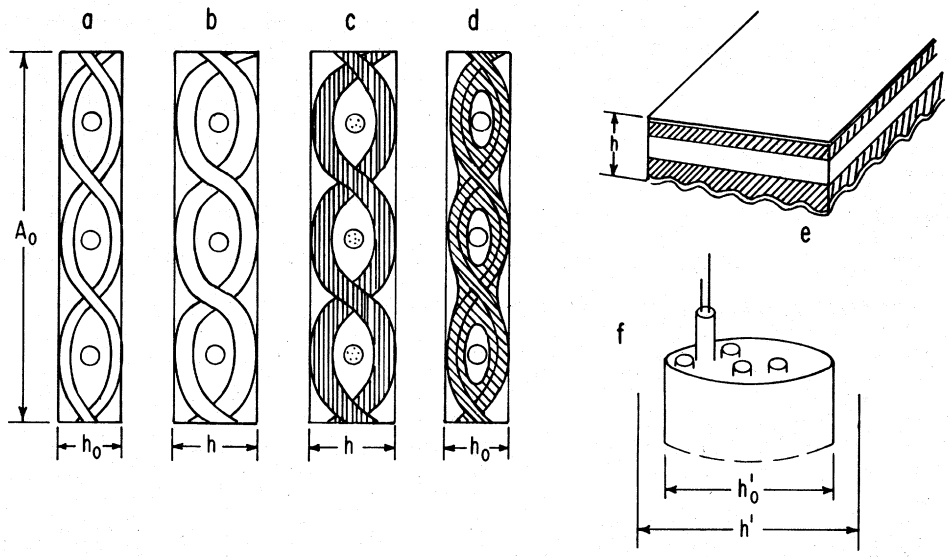

Fig. 4. Idealized models of the composites discussed in this work. Insert a, untreated 5 oz cattlehide, acetone dried, showing two fiber bundles, eq. (6); insert b, polymer deposited from emulsion, eq. (5); insert c, insert b, but after benzene extraction; insert d, location of bulk or solution polymerized monomers, eq. (7); insert e, cattlehide panel with polymer preferentially deposited in layers at grain (top) and split corium regions (bottom) but with small clear zone at surfaces; insert f, schematic of fiber bundle with polymer deposited around fibers (arrow). Fibrils are indicated in one protruding fiber; these were only occasionally surrounded.

clear zone was also observed at both panel surfaces by light microscopy observation of stained sections. In contrast, polymer deposited by bulk or solution polymerization, initiated by AIBN (insert d) was homogeneously distributed throughout the panel, which usually retained its original dimensions. Although benzene extractions removed most of the PMMA from these systems, considerable amounts (BA + MMA, 17.2% and BA, 19.2%) remained bound to the matrix, even though AIBN is a very poor initiator for grafting (36b). In these systems, incremental space filling by polymer is considered to be the only possible mode of deposition. In accordance with the models illustrated in Figure 4, the variation of composite density with composition is treated first analytically and then experimentally in the sections below.

It was shown previously (1) that the apparent density, ρ_a, of 1 g of the composite $(W_1 + W_2)$ (Fig. 4, insert b) follows the relation

$$\rho_a = 1/\{W_1/\rho_r + W_2/\rho_p + [\phi_{fo}(W_1/\rho_{ao})]\rho_{ao}/\rho_i\} \qquad (5)$$

where $W_1 = (W_1 + W_2)\, w_1$ and $W_2 = (W_1 + W_2)\, w_2$ because ρ_r is the real density of leather (1.434 g cc^{-1}), obtained with a helium air pycnometer. W_1/ρ_r is, therefore the volume of collagenous material, W_2/ρ_p is the volume of polymer, and the last term is the volume of free space remaining because ρ_{ao} is the apparent density of untreated leather (emulsion controls, 0.5556 g cc^{-1}) and ϕ_{fo} (0.6125) is the volume fraction of free space in untreated leather. The quantity ρ_{ao}/ρ_i (0.9238) is an empirical shift factor, discussed previously (1). By similar reasoning, densities for inserts a, c, and d in Figure 4 were derived (1); some of the analytical expressions are listed below. The effect of surface and partial layering on composite density (Fig. 4, insert e) was shown in Part I[1] to reduce to eq. (5) when the whole composite sample was considered. Consequently, the experimental data of this paper were correlated by means of the simple equations listed below.

insert a:

$$\rho_{ao} = 1/[W_1/\rho_r + \phi_{fo}(1/\rho_{ao})] = 1/V_T \qquad (6)$$

insert d:

$$\rho_a = 1/\{W_1/\rho_r + W_2/\rho_p + [\phi_{fo}(W_1/\rho_{ao}) - (W_2/\rho_p)\,(\rho_r/\rho_p)]\} \qquad (7)$$

$$h = V/A = [(1/W_1)/\rho_a]/A \qquad (8)$$

where h is specimen thickness in cm, V is the volume of 1 g of composite, and A is the area. This is based on no distortion of length or width as polymer deposits (1). Volume fraction of polymer follows:

emulsion:

$$\phi_2 = W_2/\rho_p/\{W_2/\rho_p + W_1/\rho_p + [\phi_{fo}(W_1/\rho_{ao})]\rho_{ao}/\rho_i\} \qquad (9)$$

bulk-solution:

$$\phi_2 = W_2/\rho_p/(W_2/\rho_p + W_1/\rho_{ao}') \qquad (10)$$

where:

$$\rho_{ao}' = 1/\{1/\rho_r + [\phi_{fo}(1/\rho_{ao}) - (W_2/\rho_p)\,(\rho_r/\rho_p)]\} \qquad (11)$$

Replica density, after dissolution of the collageneous material with hydrochloric acid (see Experimental), follows the general equation.

$$\rho_d = W_2/(V_F + W_2/\rho_p) \qquad (12)$$

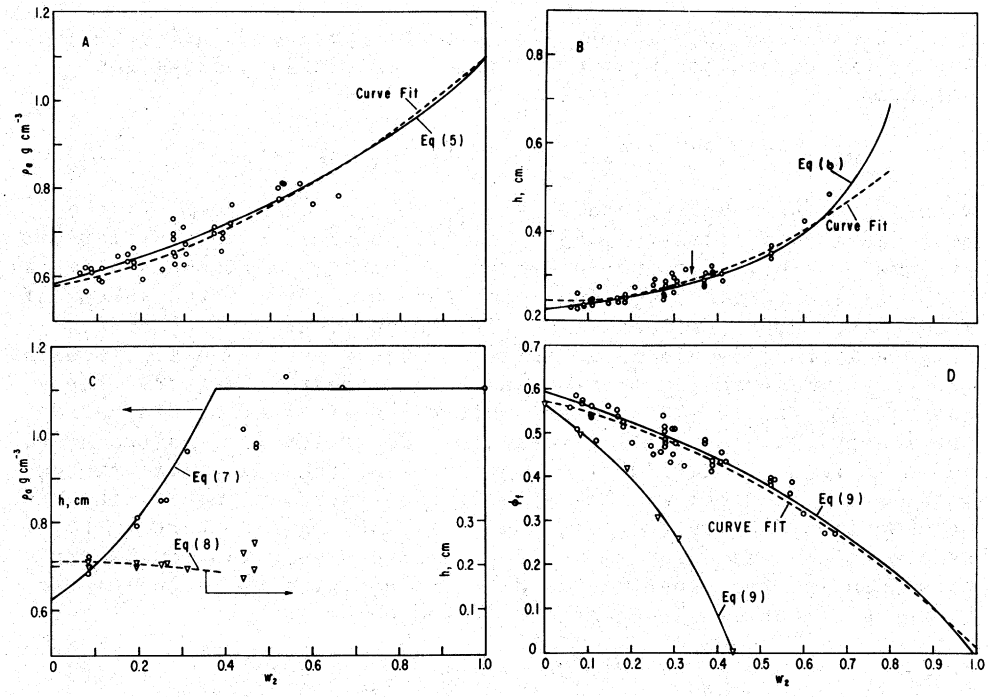

Fig. 5. Plot of apparent density, ρ_a (insert A) and specimen thickness, h, in cm (insert B) versus the weight fraction of polymer in the composite, w_2, for deposition of BA + MMA from emulsion. Plot of ρ_a and h versus w_2 (insert C) for BA + MMA composites formed by bulk or solution polymerization. Volume fraction of free space, ϕ_f, versus w_2 (insert D) for BA + MMA composites prepared by both methods.

where V_F is the sum of the volume of free space of the matrix and eliminated collagen. However, for the emulsion composites, the effect of layering had to be considered (3).

Experimental data for BA + MMA composites as a function of the polymer composition, w_2, are compared with the calculated values in Figure 5. Similar results were found for the other two systems (1). Curve fitted data (dashed lines) were close to the theoretical curves (solid lines) for insert A, densities, ρ_a (g cc^{-1}), and insert B, thickness, h (cm), versus w_2 for the emulsion systems. The more rapid rate of change of density with w_2 for the bulk-solution systems (insert C) as well as the influence of thickness is accurately predicted. Finally the difference in the rate of change of the volume fraction of free space, ϕ_f, with w_2 is illustrated in insert D for both systems. Consequently

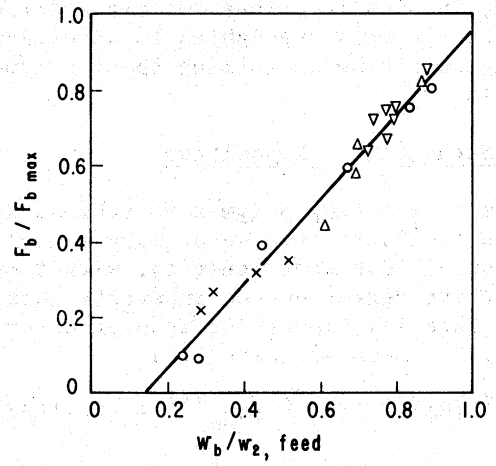

Fig. 6. The quantity $F_b/F_{b\,max}$ versus $w_b/w_{2,\,feed}$ for all three composite systems. Symbols are: circles, MMA; triangles, BA + MMA; ∇, BA + MMA, rate; x, BA.

the analysis of density, with due allowance for the natural variability of leather reflected in the considerable experimental scatter (1), confirms the behavior suggested by the models in Figure 4. Prediction of residual free space with change in composition and its proper treatment through use of volume fraction in data comparison can now be utilized.

Graft frequencies, F_b, listed in Table 1, last column, were estimated by use of eq. (3) from number-average molecular weights of the bound polymer (assuming that all was grafted). All were shown (1) to be lower than the maximum attainable, $F_{b\,max}$. The latter was calculated by eq. (3) with the feed composition. According to eq. (3), the number of chain branches, $F_{b\,max}$, should increase with w_2, becoming very large as $w_2 \rightarrow 1.0$. However, the saturation limit of polymer deposition, discussed in the Introduction, intervened. In fact, Figure 6 shows that $F_b/F_{b\,max}$ for all three systems studied approached zero before $w_b/w_{2,\,feed}$. Since the latter term is an index of grafting efficiency at 100% conversion, decreasing from right to left in the figure as monomer feed content increased, the number of branches actually formed declined at a faster rate, and thus demonstrated even more resist-

ance to forcing conditions. This argues strongly against a facile grafting mechanism. In the section below, the kinetics of bound polymer formation, in both locations, matrix and float, is treated as a function of the reaction variables to ascertain the type of mechanism actually operating in forming these polymer-leather composite materials.

B. Kinetics and Mechanism of Deposition

The mechanism of grafting polymer to fibrous surfaces is usually considered (7-12) to involve primary radical attack on substrate, terminating initiator activity, with simultaneous formation of an active center on the substrate that initiates a grafted chain. A rate law, involving assumption of homogeneous reaction kinetics, has been suggested (2)

$$R_p = k_p/k_t^{1/2}\ [M]^{3/2}\ [I]^{1/2}\ fk_{de}^{1/2} + (k_{tr}[LH])^{1/2} \qquad (13)$$

where k_p, k_t, k_{de}, and k_{tr} are specific rate constants for propagation, termination, decomposition, and transfer respectively, and [M], [I], and [LH] are the concentrations (mole $l.^{-1}$) of monomer, initiator and leather, respectively. This is similar in form to that proposed for Ce^{IV} initiation on polyols (41-46).

In contrast, the rate law for the nearly steady-state rate (interval II, conversion 5 to 50%) of polymerization in emulsion (2,47-50) is

$$R_p = -d\ [M]/dt = (k_p/N_A)(\rho_m/\rho_p)\phi_2 NQ \qquad (14)$$

where N_A is Avogadro's number, ρ, density of subscripts m (monomer) and p (polymer), respectively; ϕ_2 the volume fraction of monomer in the particle; N the number of particles; and Q the average number of radicals per particle (ideally 0.5) (47). Thus, in the ideal case, rate is proportional to only the number of particles and the monomer concentration per particle. The number of particles, N, depends on surfactant [S] and initiator concentration through (49)

$$N = 0.208\ [S]^{0.6}\ R_i/K^{0.4} \qquad (15)$$

where $R_i = 2k_{de}N_A\ [I]$ and K the volume growth rate of a particle. Equation (14) applies equally well to micellar stabilization and self-nucleation in aqueous dispersion (51,52). If the colloid particles coalesce, the limiting Case III condition applies (47) and

$$R_p = k_p[M](V_p k_{de} N_A[I]/k_t)^{1/2} \qquad (16)$$

where V_p is the total volume of the polymer particles. This equation is identical in form to the normal rate law for homogeneous polymerization.

$$R_p = k_p/k_t^{1/2} [M] [I]^{1/2} (fk_{de})^{1/2} \quad (17)$$

From the foregoing, grafting (eq. (13)) is expected to show a 3/4 power dependence on [M] and is half order in initiator and leather amount, respectively. If emulsion kinetics prevail, the exponential dependence is 0.4 in [I] and 0.6 in [S], but zero in monomer disappearance from the stabilized reservoirs in the aqueous phase (2,47-50). Consequently the exponential intensity factor, a, of the general equation for rate, R,

$$R = R_o [V]^a \quad (18)$$

where [V] is the variable concentration, should permit a choice to be made of the dominant mechanism that pertains in these systems.

The effects of the initiator concentration, [I], on rate (eq. (4)) for MMA systems are shown graphically in Figure 7. These illustrate the type of information obtained and are typical of all of the kinetic curves. The curves, starting at the top, represent the total rate, R_T, the rate of deposition, R_d, the rate of bound polymer formation, R_b, and the rate of polymerization in the float, R_f. Most of the rate data were linear to about 40-50% conversion, except R_d and R_b, which were linear to 85 to 90% conversion (Fig. 2, inserts B and C). The data were maintained therefore within the interval II (3,47-50) conversion region in emulsion polymerization. After the rate data were inserted in eq. (18), the exponential intensity factors for all of the variables were obtained and are listed in Table II. The dependence of the factor, a, on monomer concentration for MMA, (Figure 8), and BA + MMA (Figure 9), was zero because rates in both matrix and float were constant as the monomer concentration in the float varied. Thus (Table II) the effect of monomer concentration is more in harmony with the theoretical requirement of emulsion polymerization than that expected of a dominant grafting mechanism. Similarly the dependence of a for R_d on [I] and [S] exhibits more typical emulsion polymerization behavior. However, the anomalously large value of a for R_d as a function of [I] is clear evidence of a gel effect (36b), which would be expected as the polymer particles coalesce on being deposited in the leather matrix (2,3), thus trapping radicals and lengthening their lifetimes. In the absence of leather, a became closer to theory. In contrast, R_b showed erratic behavior and much experimental scatter (2) in plots based on eq. (18). This suggests that the bound polymer was patterned from the deposition rate as a secondary consequence and was not the guiding mechanism as specified by eq. (13). While the initial

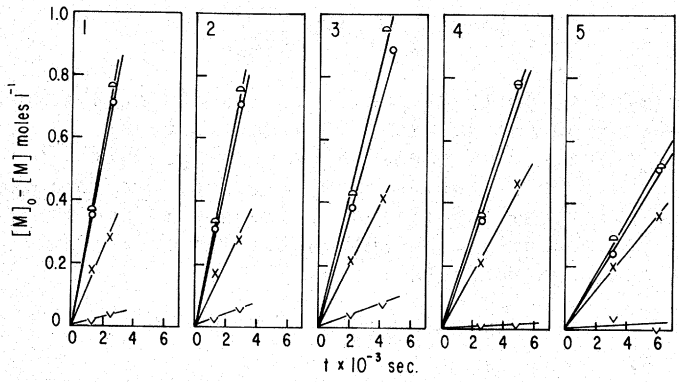

Fig. 7. Rate of monomer consumption versus time for the MMA composite systems of Table 2 at varied initiator concentrations. The order of the rate curves in each insert, top to bottom, is: R_{T1} R_d, R_b, R_f. Initiator concentrations are, in mole l^{-1}: insert 1, 0.1945; insert 2, 0.1552; insert 3, 0.0750; insert 4, 0.0582; insert 5, 0.0402.

rates all showed an apparent dependence on leather amount (Table 2 and Fig. 2, inserts B, C, D), the magnitude of a decreased rapidly to nearly zero (Table 3) after 1 hr reaction for BA + MMA and BA systems. As seen in Table 3, the total rate of polymerization, R_T, became constant with [LH] in this interval, when conversions were only around 17%. Consequently the amount of leather initially present had no permanent influence on rate for these systems. The apparent accelerating effect of [LH] on MMA systems may have resulted from strong Tromsdorff retardation of k_t in the highly viscous MMA polymer aggregate.

From the foregoing, a mechanism of deposition that proceeds from the observed dependence on emulsion kinetics through eq. (14) is suggested as an alternative to grafting. Polymer first appears in particles in micelles or by self-nucleation (51,52) in the float and in the aqueous phase of the leather matrix. However, more polymer forms initially in the matrix because of preferential migration of persulfate ion during the reaction (2,53). Growing particles in the matrix and those entering from the float coalesce and trap radicals. The embryo deposit grows by diffusion of monomer from the surfactant stabilized monomer reservoirs, through

Table 2. Exponential Intensity Factor, a, for All Composite Systems

Reaction variable, Moles l^{-1}	Intensity constant, a							
	Emulsion theory eqs. (14) and (15)	Graft theory eq. (13)	MMA		BA + MMA		BA	
			R_d	R_b	R_d	R_b	R_d	R_b
[I]	0.4	0.5	0.723	0.444	0.657	0.841	-	-
[M]	0	1.5	0	0	0	0	0	0
[L]	0	0.5	0.885	1.05	0.636→0[a]	0.745→0[a]	0.667→0[a]	0.702→0[a]
[S]	0.6	0	0.509	0.294	0.494	0.480	-	-
[I] no. lea.					0.500			
[M] no. lea.					0			
[S] no. lea.					0.793			

[a] Dependence of the total polymerization rate, R_T, decays to 0 by an average of 17% conversion; initial $R_d = R_T$. See Table III.

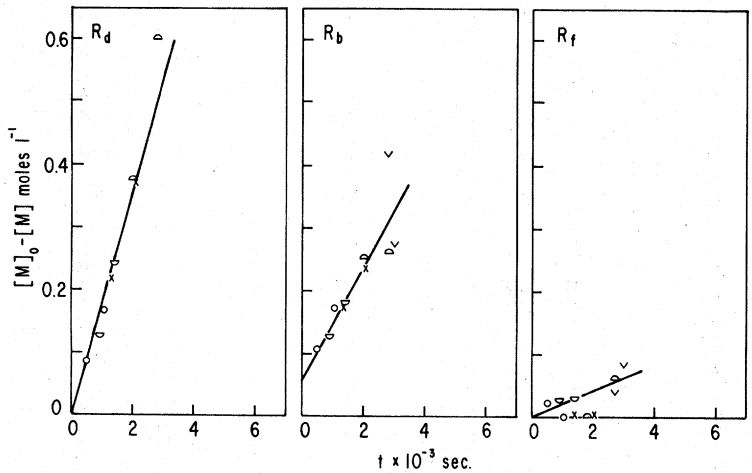

Fig. 8. Rate of monomer consumption versus time for the MMA composites with monomer concentrations varied. The MMA concentrations used were: Θ, 0.487 mole l^{-1}; ∇, 0.816 mole l^{-1}; x, 1.28 mole l^{-1}; Δ, 1.92 mole l^{-1}; v, 0.485 mole l^{-1}; all based on water.

the polymer layer, and is polymerized by the occluded radicals. In the present work, 20 to 50% of the bound polymer resulted from microgel formation. However, a considerable amount most probably resulted from strong adsorption to collagen surfaces. It is now known (5d) that ordered layers of up to 7000 A can form near surfaces and become immobilized. These are difficult to remove. This adsorption can thus contribute an enhancement to the high tortuosity of solvent diffusing through filled polymers. Thus, in the time scale of most extractions (35) much polymer would be retained. Finally, actual grafting at fiber-polymer interfaces would contribute a small amount of bound polymer.

The data in Table 4 provide additional evidence for this mechanism. The preferential migration of initiator, as reflected in the quantity $[I]/[I]_o$ (2), was higher for MMA and BA + MMA systems following a 30 min conditioning period than the statistical ratio (0.28). However, the initial equilibrium adsorption of BA + MMA monomer by the collagen matrix was less than the statistical amount. Consequently, insufficient monomer was initially imbibed into the matrix to support much grafting. In contrast, when preformed BA + MMA emulsion polymer was impregnated into the

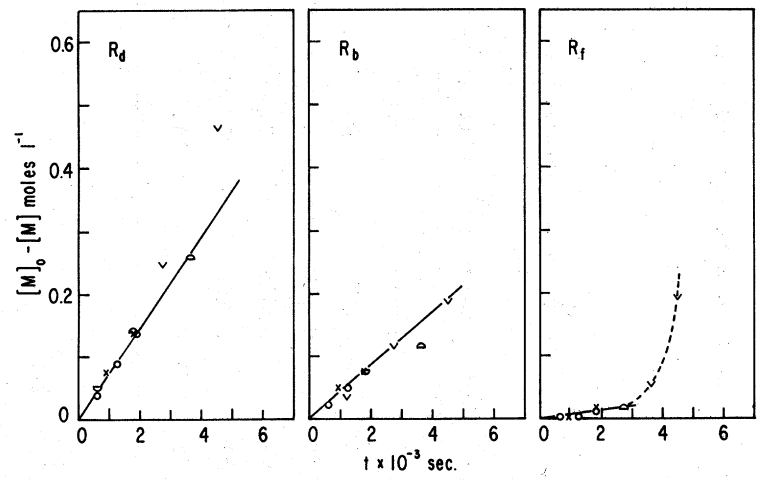

Fig. 9. Rate of monomer comsumption versus time for the BA + MMA composites with monomer concentrations varied. The BA + MMA concentrations used were Θ, 0.432 mole l^{-1}; ∇, 0.746 mole l^{-1}; x, 1.096 mole l^{-1}; Δ, 1.70 mole l^{-1}; v 3.34 mole l^{-1}; all based on water.

hydrated leather matrix, under standard conditions, about 50% of this was bound. This provides strong support for polymer adsorption because covalent bonding was impossible under the experimental conditions used. Because rates of deposition were unaffected by monomer amount, the ratio $R_d/[M]$ can be used to yield a proportionality constant that has first order dimensions (column 2). The effect of using ground leather on the magnitude of this constant is shown in the last three columns. Although the deposition rate appeared to be large in a concentrated system close to standard conditions for intact leathers, the physical state was that of a thick paste (2), ideally suited for polymer entrapment. At high dilution, most activity was tranferred to the float. For both concentrations, gel effects were greater than for initial leathers. Because grinding should have enhanced bound polymer formation if grafting were dominant because of the greater collagen surface exposed, these results are also at variance with this type of mechanism.

Diffusion control of monomer transport through the polymer layer gains credence from Figure 10. Insert A shows that the system deposition constants, D_e, of Figure 1 are directly propor-

Table 3. Effect of Leather Amount [LH] on the Initial Total Polymerization Rate and the Rate after One Hour of Reaction

MMA			BA + MMA			BA		
$R_T \times 10^5$ moles l sec^{-1}			$R_T \times 10^5$ moles l sec^{-1}			$R_T \times 10^5$ moles l sec^{-1}		
[LH] moles l^{-1}	initial[a]	1 hr[b]	[LH] moles l^{-1}	initial[a]	1 hr[b]	[LH] moles l^{-1}	initial[a]	1 hr[b]
1.96	16.5	18.2	1.96	8.40	8.96	1.98	5.00	5.56
1.37	11.0	13.6	1.34	6.50	7.61	1.26	4.00	5.67
1.03	8.50	10.4	1.02	5.45	8.78	0.960	3.00	5.08
0.690	6.17	6.95	0.711	4.08	8.94	0.625	2.40	7.26
0.319	3.20	3.62	0.341	2.75	8.31	0.302	1.45	4.81
0	2.10	2.10	0	8.25	9.75	0	14.0	27.8

[a] $R_d = R_T$ initially, because $R_f = 0$.

[b] In 1 hr the average % conversion was: MMA, 17.3; BA + MMA, 19.2; BA, 13.9.

Table 4. Steady-state Rate Constants, Initiator Distributions, Monomer and Polymer Impregnation Results, and Effect of Ground Leather on Polymerization Rate

			Leather impregnation, pre-formed polymer			Leather impregnation, monomer		Deposition in ground leather		
System	$k_d \times 10^5$ sec^{-1}	$[I]/[I]_o$,[a] After 30 min	$[P_d]$[b] moles l^{-1}	$[P_b]$ moles l^{-1}	$[P_d]/[P_T]$	$[M_d]$[c] moles l^{-1}	$[M_d]/[M_T]$	$k_d \times 10^5$ sec^{-1}	$k_f \times 10^5$ sec^{-1}	$k_T \times 10^5$ sec^{-1}
MMA	8.81	0.692								
BA + MMA	4.58	0.740	0.193	0.103	0.118	0.103	0.0644			
BA	3.56									
Powd., conc.[d]								22.1	6.18	28.0
Intact, conc.[d]								4.53	4.72	8.02
Powd., dil.[d]								4.15	32.5	40.4
Intact, dil.[d]								1.45	9.69	11.8

[a] [I] is the initiator concentration in the leather; the statistical ratio is 0.277.

[b] Initial polymer concentration in the emulsion was 1.638 Ml^{-1}. $[P_d]$ and $[P_b]$ represent the average polymer concentrations found for six impregnation experiments, of varied times between 0.5 and 5 hr.

[c] Initial monomer concentration in the emulsion was 1.638 moles l^{-1}.

[d] BA + MMA monomer. In the concentrated systems, monomer concentration was 1.13 moles l^{-1}; dilute systems, 0.277 moles l^{-1}; standard conditions, 1.67 moles l^{-1}.

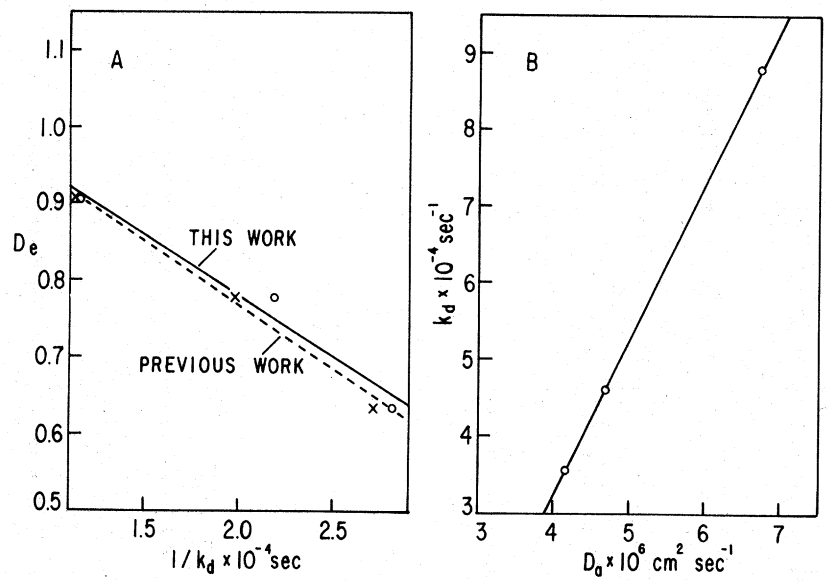

Fig. 10. Relation (insert A) between the system efficiency constant, D_e, and $1/k_d$ of this work (from Table 4) and that calculated from the data in Table 3 of a previous work.[1a] Insert B illustrates the relation between k_d of this work and the apparent diffusion constant, D_a, for the monomers through a BA + MMA panel. Values of D_a x 10^6 cm^2 sec^{-1} were: MMA, 6.72; BA + MMA, 4.69; BA, 4.16.

tional to the reciprocal of the deposition rate constants k_d from Table 4. The observation that k_d was directly proportional to the diffusion constants for the three monomers through BA + MMA film (insert B) suggests that most of the monomer arrived at the active center by passage through the deposited polymer. The preference of the polymer for the outer layers of the matrix (Fig. 4, insert e) appears to be regulated (Fig. 11) by the mean diffusive path, L in cm. This quantity approaches a limiting value when plotted as a function of the experimental layer thickness, h_p, in cm, for all three systems, in spite of considerable differences in the rates of deposition of the monomers used. The data for Figures 10 and 11 do not include tortuosity effects (5d). Use of a BA + MMA film as a model for the plasticized deposited polymer can, of course, lead to errors. However, these are considered to be small if only qualitative significance is attached to the results and when compared against those of other types of possible monomer transport.

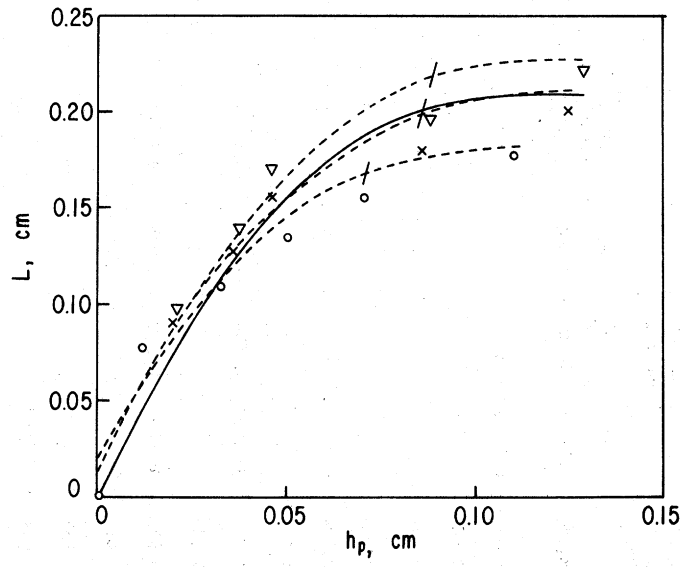

Fig. 11. Mean diffusive distance, L, versus the overall polymer thickness in the composite, h_p, as a function of time. Symbols are: θ MMA; x, BA + MMA; ∇, BA. Solid line is the average for all data. Slash marks designate the limiting h_p corresponding to the termination of significant deposition for each system.

C. Morphology of the Deposited Polymer

Extensive use has been made of the light (13,54,55) transmission (7,9,14,56-62) and scanning electron microscopes (63) in elucidating the structure of polymer composites of cotton, rayon, and wool. In both cotton (14) and wool (9), transmission electron microscopy (TEM) revealed that polymer could, by proper choice of reaction conditions, be deposited through all regions of the fiber cross sections, residing, in some cases, even around microfibrils in wool (64) to produce domains as small as 20 A thick (9). The ultrafine regions of goat skins, presumably in the vicinity of protofibrils, have been said to be permeated by depositing polymer (65), but some doubt remains concerning this interpretation (1,3).

Replica densities as functions of composite polymer composition, w_2, are shown in Table 5, together with the extent of replica shrinkage relative to the initial composite volume. Also included

Table 5. Replica Densities, Extent of Replica Shrinkage, and Rates and Water Absorbtivities of the Composites and Their Controls

Expt. no.	System	w_2	Replica density: ρ_d calc.[a] g cc^{-1}	Replica density: ρ_d found g cc^{-1}	Fractional extent of shrinkage[b]: V_r/V_{ro}	Fractional extent of shrinkage[b]: ϕ_f/ϕ_{fo}	Rates of water absorption[c]: w_s 5 sec	Rates of water absorption[c]: w_s 10 min	Rates of water absorption[c]: w_s 8 days	Equil.[d] absorb. w_{max}/w_{so}
	Poly (Methyl Methacrylate) - Leather Composites and Replicas									
1*	emuls., b.[e]	0.447	0.490	0.483	0.938	0.826				
2	"	0.335	0.363	0.345	0.900	0.916				
3	"	0.203	0.236	0.326	0.783	0.865				
4	"	0.0894	0.104	0.280	0.458	0.774				
5	emuls., d.	0.470	0.543	0.453	0.995	1.02				
6	"	0.347	0.402	0.381	0.963	1.03	0.300	0.550	0.593	1.05
7	"	0.258	0.300	0.308	0.942	0.938				
8	"	0.182	0.212	0.250	0.871	0.949	0.536	0.570	0.605	0.967
9	emuls., a.	0.447	0.517	0.433	1.01	1.01				
10	"	0.366	0.424	0.410	1.04	0.955				
11	bulk, d.	0.423	0.535	0.423	1.03	0.995				
12	"	0.292	0.272	0.288	0.989	0.975				
13	"	0.234	0.199	0.219	1.01	0.995				

14	"	0.189	0.145	0.180	0.942	0.977	0.240	0.440	0.494	1.06
15	"	0.155	0.118	0.202	0.768	1.01				
16	"	0.397					0.175	0.205	0.339	1.87
		n-(Butyl Acrylate-co-Methyl Methacrylate) - Leather Composites								
17	emuls., d.	0.189	0.404	0.262	0.857	0.821	0.040	0.550	0.591	1.03
18	"	0.304	0.436	0.420	1.07	1.09	0.200	0.525	0.590	1.04
19	bulk, d.	0.174					0	0.510	0.570	1.22
20	"	0.310					0	0.130	0.480	1.54
		n-(Butyl Acrylate) - Leather Composites								
21	emuls., d.	0.208					0	0.300	0.527	0.902
22	"	0.303					0	0.440	0.525	0.910
23	bulk, d.	0.143					0	0.120	0.433	0.884
24	"	0.281					0	0.095	0.408	1.17
		Average of All Controls								
25	-	0					0.526	0.544	0.590	0.966

[a] Eq. (12).

[b] V_r is the measured volume of the replica and V_{ro} that of the original composite, but thickness for both was calculated by eq. (8). The volume fraction of replica free space is ϕ_f, given by V_a/V_T from replica density; ϕ_{fo} is 0.6125.

(continued)

Table 5 (continued)

[c] w_s is the weight fraction of water adsorbed.

[d] w_{max} is the weight fraction of water absorbed after 8 days; w_{so} is $\phi_{fo}\ \rho_w$, where ρ_w is the density of water at 23°C.

[e] Letters designate, bound polymer, b; deposited polymer, d.; and air-dried, a.

* Denotes sample used for micrographs.

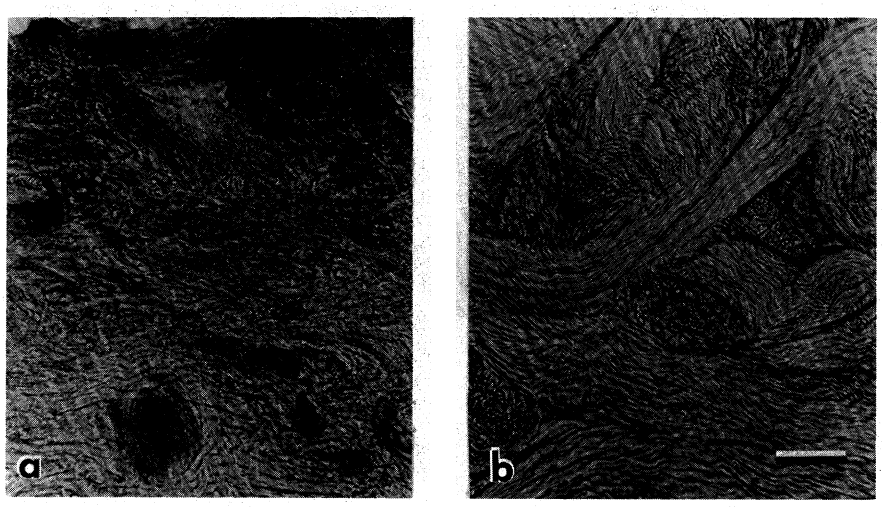

Fig. 12. Light microscope (LM) micrographs of untreated 5 oz chrome-tanned cattlehide (control) showing cross sections of portions of the grain layer (insert a) and the corium layer (insert b). The lower half of insert a is the grain-corium interface region. The dark circular area is the root of a hair follicle; the other irregular dark areas are fragments of capillaries or fatty deposits. The scale is 100 μm.

are significant time increments for the rates of water absorption (columns 8, 9, 10) and the equilibrium water absorptivity (last column) for composites compared with their controls. While replica densities, both calculated (eq. (12)) and found, decreased as w_2 decreased, the rate of change was less for the emulsion system at each w_2 increment than for the bulk-solution systems, reflecting the greater exhaustion of the space brought about by concentrating the polymer in layers. Shrinkage by both methods of composite preparation was generally small (columns 6, 7) especially for experiments 5 through 17. Thus the micrographs of the replicas should reflect the actual morphology of the continuous polymer phase present in the composites before fiber removal. Figure 12 presents light photomicrographs of untreated controls at 40X (100 μm) for, the grain (top) and transition region below (insert A), and the corium region below that in insert A (insert B). The dense finely structured grain fibers and fiber bundles contrast with the much coarser, more articulate fiber bundles. Individual

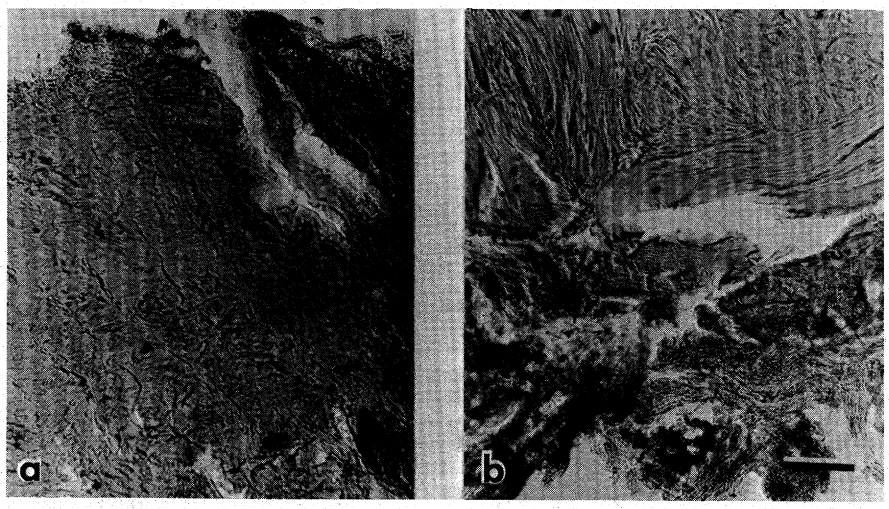

Fig. 13. LM micrographs of the cross sections of the replicas prepared by hydrochloric acid etching of the composites made from the untreated leathers in Figure 2. Insert a is the grain layer; insert b is the corium layer. The scale is 100 μm.

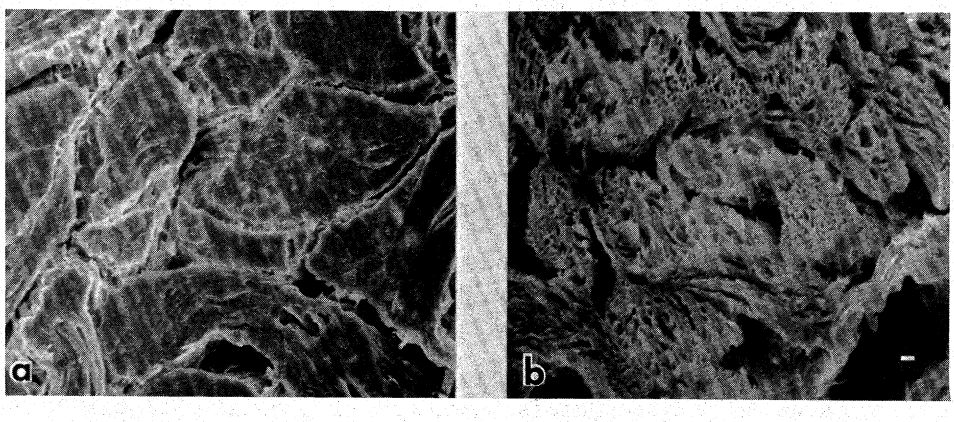

Fig. 14. Scanning electron micrographs (SEM) of cross sections of bound polymer-leather composites, prepared in emulsion (Table V), insert a, and the corresponding replica, insert b, prepared by hydrochloric acid etching, showing the effect of removing the collageneous material, selected from similar regions of the corium. The scale is 10 μm.

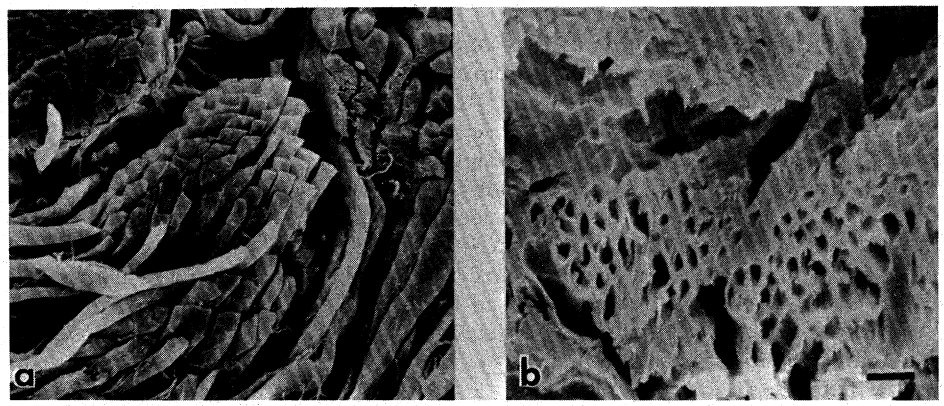

Fig. 15. SEM of a cross section of untreated leather (insert a) at higher magnification (1,000X) than that of Figure 14; insert b (300X), compared with a typical section of the bound polymer replica (insert b) of Figure 14. Fiber diameters correspond approximately to replica openings; the polymer is largely confined to the fiber bundle. The scale is 10 μm.

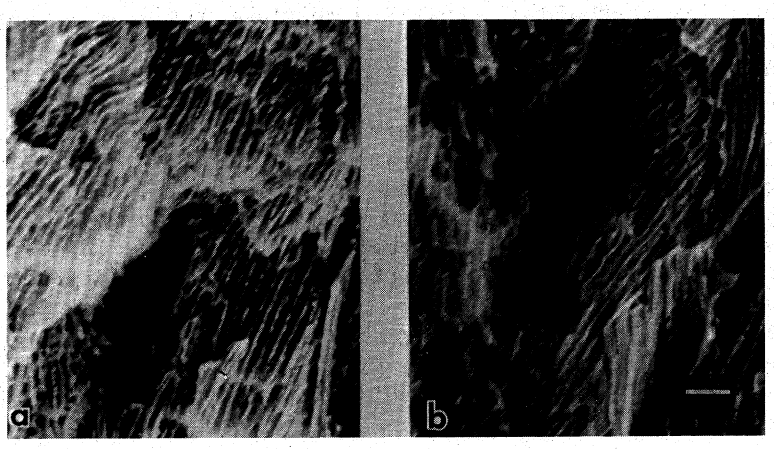

Fig. 16. High magnification (10,000X) SEM of the cross section of the corium region of a replica of a composite (Table 1, exp. 1) inserts a and b were taken from different positions in the replica. The linear hollow tubes are approximately 500 to 2,000 Å in diameter and correspond to the dimensions of fibrils. The scale is 1 μm.

fibers can be seen as fine striations in the micrographs. Corresponding replicas of the bound polymer (experiment 1, Table 5)

from grain (insert a) and corium (insert b) in Figure 13 reflect this fiber morphology but still reveal the plastic character of the deposit. Scanning electron micrographs (SEM) of the cut surfaces of the same composites (Fig. 14, insert a) showing the expanded fiber bundles with polymer packed around individual fibers (shown schematically in Figure 4, insert f), which, when removed by dilute acid (insert b) reveal holes and tubes 1.5 to 4 μm in diameter in the replica, corresponding to typical fiber diameters. This can be seen better in Figure 15 where, at higher magnification (1000X), openings of the fiber diameter are readily seen. Because these openings were not larger than initial fiber diameters (insert a) and the visible polymer corresponded closely with the composite weight fraction, most of the polymer deposited around fibers in coarse domains, 2 to 50 μm. In this way, fiber bundles expanded to produce the matrix expansion discussed in terms of models in Figure 4. However, some polymer in the emulsion systems did penetrate to lower aggregation levels. Figure 16 shows replicas at 10,000X that reveal tubular traces 300 to 800 Å originally surrounding fibrils, which had typical diameters of 500 to 2000 Å. Other features of the morphology of these composites illustrated by use of SEM in a more thorough study (3) revealed an extremely complex morphology. As polymer composition in the composites was reduced, all replicas became more porous but possessed similar morphology. Bulk and solution replicas appeared to be rather dense, especially at high w_2, because polymer resided in large pores. However, it was excluded from the interfibrillar regions. Air-dried or methanol-dried replicas revealed partially aggregated colloidal polymer spheres, 2000 to 10,000 Å in diameter, clustered on fused polymer aggregates. These were the original emulsion particles before coalescence. In general, the micrographs revealed a morphology in harmony with the idealized models in Figure 4 and with the deposition mechanism set forth in section B above. The influence of this morphology on water absorption was also considered.

The rate of water absorption by the untreated control in Table 5 (average values, experiment 25) followed the simple relation (3)

$$w_s = w_{si} + k \ln t \qquad (19)$$

where w_s is the weight fraction of water absorbed by the sample, w_{si} is the instantaneous (1 sec) weight fraction of water imbibed, k is a constant (0.00670 sec^{-1}), and time, t, was followed up to 8 or more days. Rates for the composites were estimated by computing a corrected absorption weight fraction, $w_{s\ corr.}$, (from w_s in eq. (19)) to the state of pure collagen by use of $w_{s\ corr.} = f_s/w_1$, where $f_s = W_s/(W_1 + W_2)$ is the observed fractional water absorption. Rate became vanishingly small after 8 days.

Table 6. Selected Mechanical Properties of Poly-(Methyl Methacrylate)-Leather, Composite Materials

Expt. no.	Composition		Tensile strength		Initial tensile moduli		Torsional moduli, methanol-dried		Torsional moduli, air-dried	
	w_2	ϕ_2	TS, psi	TS/TS_1	E, psi	E/E_1	E_t, psi	E_t/E_{t1}	E_{t1}, psi[a]	E_t/E_{t1}
1	0	0	1,722	1	1,290	1	1,944	1	32,000	1
2	0.0807	0.0423	1,275	0.970	3,450	2.60	2,050	1.37		
3	0.103	0.0543	1,725	1.03	5,550	4.18	1,300	1.33	31,200	0.577
4	0.182	0.0992	1,810	1.03	5,100	3.84	4,500	4.50	38,800	0.443
5	0.235	0.131	1,220	0.649	50,600	45.2	14,000	11.2		
6	0.258	0.145	1,560	0.650	8,980	5.51	7,800	5.20	26,500	0.891
7	0.347	0.202	1,215	0.631	9,840	9.93	4,800	4.00	32,000	1.10
8	0.470	0.288	1,395	0.542	41,400	20.5	29,000	20.3	39,500	2.61
9	0.504	0.314	2,170	1.28	65,400	76.0	44,000	33.8		
10	0.657	0.439	918	0.461	39,400	25.2	37,000	30.8	51,000	3.63
11	1.0	1.00	7,760	4.51	220,000	165.7	540,000	27.8		

[a] Approximate relative torsional stiffness for all three polymer systems at $w_2 \sim 0.25$ were: MMA, 1; BA + MMA, 0.386; BA, 0.342; controls 0.139.

[b] Corresponding composite w_2 and ϕ_2 were: expt. no., w_2, ϕ_2; 1, 0, 0; 3, 0.127, 0.069; 4, 0.186, 0.104; 6, 0.298, 0.170; 7, 0.342, 0.199; 8, 0.478, 0.292.

Consequently, this was the time usually taken for equilibrium absorption in Table 5. Because it was shown (3) that wet densities remained constant after 2 sec (1.09 $g \cdot cc^{-1}$) the matrix expanded in proportion to the water imbibed. A limiting weight fraction of water absorbed, w_{so}, could therefore be computed from $\phi_f \rho_w$, where ρ_w is the density of water at 23°C and ϕ_f the volume fraction of free space in the emulsion composites, obtained by rearranging eq. (9). The ratio, $w_{s\,max}/w_{so}$, with w_{max} the observed equilibrium weight fraction of water absorbed in 8 days is an index of the effectiveness of deposited polymer in preventing water absorption in these composite materials. When the ratio is unity, no shielding of collagen occurs; values <1 indicate reduced absorption and values >1, enhanced absorption. For bulk or solution composites, w_{so} tended to be underestimated because of the rapid decline of ϕ_f with w_2 increase (Fig. 5, insert D). Because $w_{s\,max}$ should increase normally here since interfibrillar regions were free of polymers (3) the observed ratios (Table 5) may have increased abnormally.

Results in Table 5 show that in the emulsion systems polymer presence slowed the rate of absorption (rate data to be compared with that of experiment 25). The rates were much slower in the bulk-solution process, than in the emulsion process; some systems (experiments 14, 16, 20, 23, 24) did not reach equilibrium even after 8 days. In contrast, the equilibrium absorption index ($w_{s\,max}/w_{so}$) was nearly always unity for the emulsion systems, but was abnormally high for certain bulk systems (experiments 16, 19, 20, 24), for reasons discussed above. It may be concluded that when polymer is deposited in leather by either process, little permanent protection was observed from imbibed water under static conditions.

D. Mechanical Properties

The mechanical properties of cotton and wool and other natural fibers and fabrics containing grafted and deposited polymers have been discussed as part of reviews (4,7,9,12). In general, for treated cotton fibers, tenacity (13,57,60,61,66-67), break toughness (57,60,61,66-67), and stiffness (13,57,60,61,66-67) generally decreased, while elongation remained constant. Flex and flat abrasion resistance for fabrics was greatly improved (68-70). Similar behavior was observed for wool fibers (9,71-74) and fabrics (55,74). While many mechanical properties of leathers have been reported (75-76), including the effect of natural variability (77-79), the mechanical properties reported on polymer grafted composites have been largely limited to the determination of tensile strengths (4,80,81).

The mechanical properties selected for this work were limited to the MMA systems in Table 6 and were specifically restricted to methanol extracted and air-dried composites. Similar data were

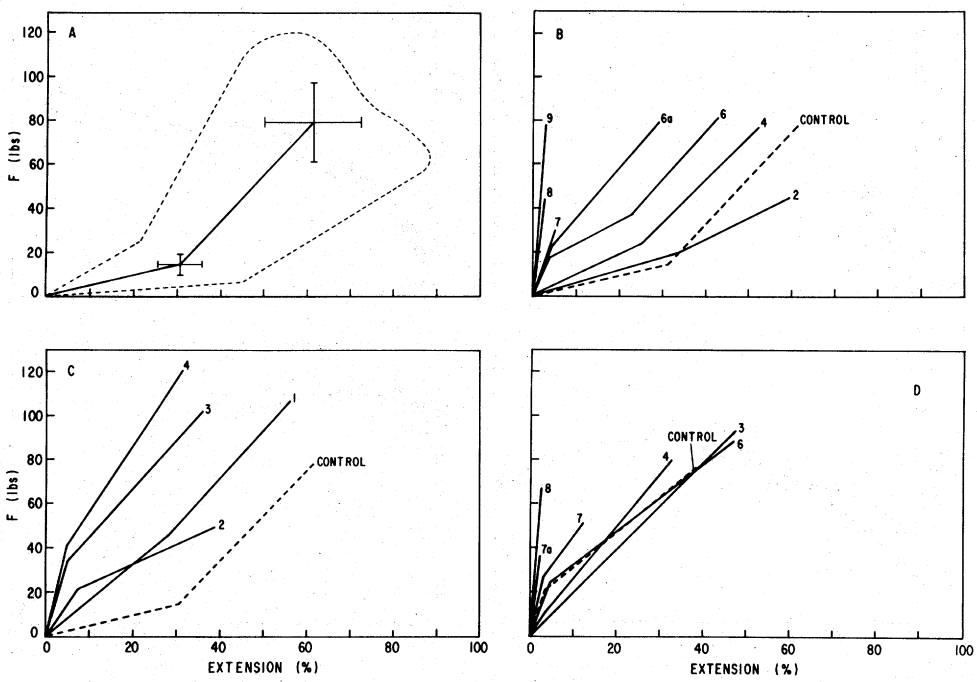

Fig. 17. Simplified force-extension curves. Insert A, averaged curve for all untreated controls. The bars designate standard deviations of both force and extension for each linear region and the dotted envelope is approximately the extreme limits observed. Inserts B (MMA) and C (BA + MMA), curves for emulsion prepared composites, methanol extracted only. Insert D, air-dried composites (solid lines) and the average curve for air-dried controls (analogous to insert A) dashed line. Numbers in inserts B and D correspond to those in Table 6. Insert C, exp. no., w_2: 1, 0.0875; 2, 0.280; 3, 0.389; 4, 0.523.

observed (4) for the BA + MMA and BA composites. Results on those systems not listed in Table 6 are treated in the figures below. Although tensile strengths did not decrease appreciably when compared to the average of the controls (experiment 1), natural variability of the controls was great. Consequently, the relative tensile strengths TS/TS_1, which compare the TS of each composite with that of its control, yielded more reliable information. Tensile strengths tended to decline with composition for the MMA systems here, but the relative values were larger for BA + MMA and BA (4). Tensile and torsional stiffness increased appreciably with increase in polymer content, both absolutely (columns 6 and 8) and relatively (columns 7 and 9). However, simply air-drying the controls (column 10) greatly increased their stiffness. This

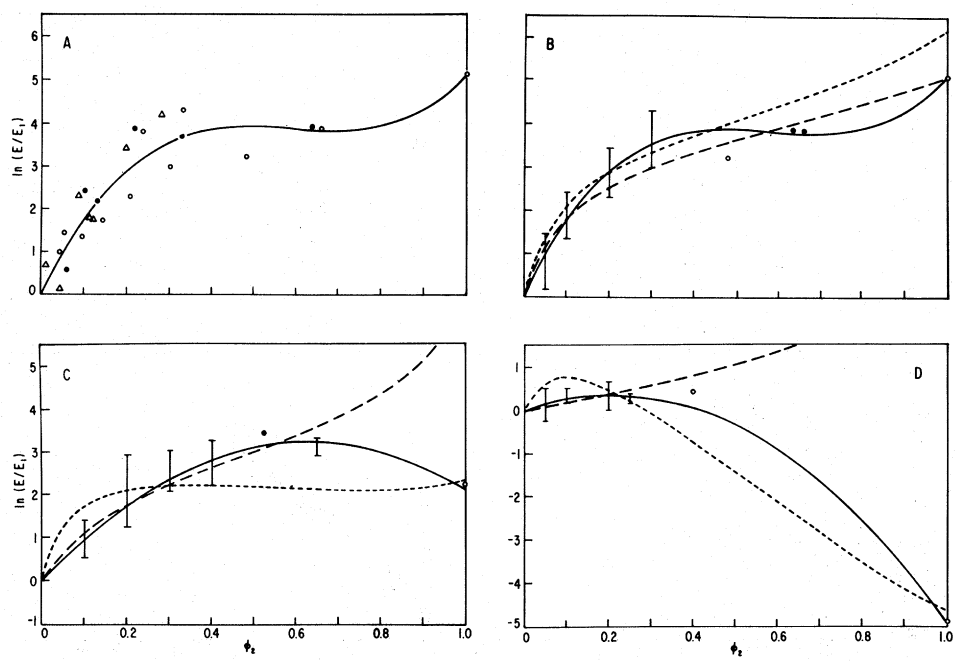

Fig. 18. The log of the modulus ratio in tension ln (E/E_1) for composites relative to their controls, (E_1), versus the volume fraction of polymer in the composite, ϕ_2. Insert A computer fitted curve (eq. (9)) drawn through all MMA data. Symbols are: circles, methanol extracted, triangles, benzene; filled circles bulk-solution. In inserts B (MMA), C (BA + MMA), and D (BA), curves were fitted by computer (solid lines) and by constants of the Halpin-Tsai equation (eq.(20)) (dashed line) and the modified Halpin-Tsai equation (eq. (22)) (dotted line). The bars represent the extremes of the experimental scatter.

was thought to arise from aggregated fibers, accompanied by distorted initial fiber conformations and reduction in free space. Average densities did, indeed, increase from 0.556 to 0.649 g cc^{-1}. Polymer presence reduced some of this aggregation because relative moduli now generally decreased (last column). Thus, a morphology consisting of polymer residing mostly around fibers in fiber bundles, as was observed in section C, functions the same way mechanically as generally aligned fibers and fiber bundles obtained through shrinkage of the fibrous matrix.

The reason for the tensile stiffness behavior is illustrated in Figure 17. The schematicized average force-extension curves

for all of the untreated leather controls are drawn in insert A. The natural variability was extreme as shown by the mean deviations (bars) and the extremes of variability (dotted envelope) but is typical of leather (77-79). Curves for composites of MMA (insert B) and BA + MMA (insert C) of varied w_2 are compared with this average control tensile (dashed line).[2] Clearly the initial modulus increased with increase in polymer composition. Noteworthy is the discontinuous shift in curve shape at w_2 ~0.2 for both systems. Analogous behavior was found for the average of the air-dried controls (MMA) dashed line in insert D, where curves for composites and their controls were similar. Relative tensile moduli at ambient temperature (composite/control) for all experimental data, regardless of treatment (methanol extracted or benzene extracted) or method of preparation (emulsion or bulk solution) are plotted (Fig. 18) as functions of the volume fraction of polymer, ϕ_2, the latter computed by use of eqs. (9) or (10). All data fell randomly near a common computer fitted curve (solid line, insert A). Consequently, both methods of preparation and all subsequent treatments yielded similar mechanical response. However, experimental scatter, resulting largely from natural variability of the leather (Fig. 17, insert A) was so excessive that all relationships must be considered to be only qualitative. Curve fitted relative moduli (solid lines) are shown for MMA composites (insert B), BA + MMA composites (insert C), and BA composites (insert D). These curves illustrate that, at increasing ϕ_2, a contribution of the viscoelastic response of the specific modifying polymer became important and finally dominated properties at ϕ_2 approaching unity. The dashed line was drawn (4) by use of the Nielsen modification (82a,b) of the Halpin-Tsai equation.

$$E/E_1 = (1 + AB\phi_2)/(1-B\psi\phi_2) \qquad (20)$$

In this equation, the constant A accounts for the geometry of the filler and Poisson's ratio of the matrix. The constant A increases greatly as the filler geometry changes in shape from spheres, to rods, to fibers (82a), and approaches an upper bound for a morphology of aligned fibers (parallel packing). The constant B, on the other hand, is sensitive to the relative moduli for both components, approaching zero as E_2/E_1 approaches ∞.

$$B = [(E_2/E_1)-1]/[(E_2/E_1) + A] \qquad (21)$$

Finally, the quantity, ψ, is related to the maximum packing volume, ϕ_m (82a). Because phase inversion was never found (82a) in this work, ψ was assigned a value of unity. For use of eq. (20), the modulus of the untreated leather (designated to be E_1, eq. (20)) was useful only as a predictive equation for the MMA composites (insert B). For this system, the magnitude of the constant A (70.4) (4) clearly indicated generally parallel packing. This is

in line with a model (Fig. 4) wherein parallel packed fibers of the leather matrix are restricted in their movement by polymer encasement. The fit for the other two systems, inserts C and D, which involved an unrealistic assignment to B (4), relegated these to mere empirical correlations of limited utility.

Similar results were found for computer fitted relative torsional moduli ratios, solid lines in Figure 19, for MMA (insert B), BA + MMA (insert C), and BA (insert D). Again the Halpin-Tsai relation (eq. (20)), dotted line, was predictive only for the MMA composites. Relative moduli, similar to those for the stiff MMA composites in insert B, were obtained (insert A) for untreated air-dried control samples (Table 6) fitted by use of eq. (20) versus the fractional increase in density $(\rho_a - \rho_{a1})/(\rho_{a2} - \rho_{a1})$. Constants were: A, 268.2; B, 0.625. In view of the common mechanical behavior illustrated in inserts A and B, where fiber aggregation and polymer impregnation produced curves of similar shape, an equation was proposed (4) that linked the initial stiffness produced by permeating polymer at low ϕ_2 (as fiber movement was initially restricted, and free space depleted (Fig. 5, insert D) with the situation at higher ϕ_2 where the viscoelastic properties of the modifying polymer became manifest. For this, the constants A and B for air-dried controls were inserted in a modified Nielsen-Halpin-Tsai equation, given as (4)

$$E_t/E_{t_1} = [(1 + AB\phi_2)/(1 - A\psi\phi_2)] + C\phi_1 + \phi_2 \ln(E_h/E_c) \qquad (22)$$

where $C = K\ln(E_h/E_c)$, K is a constant and E_c and E_h are the modulis of collagen and the modifying polymer, respectively (4). With small alterations of the adjustable parameters, $C\phi_1$ and ϕ_2, curves obtained by use of eq. (22) were drawn (Figure 18, dotted line) for MMA composites (insert B) BA + MMA composites (insert C) and BA composites (insert D). Similarly, curves were drawn (Figure 19, dashed lines) for MMA, BA + MMA, and BA composites in inserts B, C, D, respectively. Although the fit in Figure 19 is better than that in Figure 18, both predict only qualitatively the main features observed for ambient moduli for all of the experimental data in this paper, regardless of method of preparation or of subsequent treatment. Because the glass transition temperature (T_g) of the modifying polymers was selected to have a wide variation, eq. (22) should be useful in predicting relative moduli for many different polymers. In fact, variants of eq. (22) might have predictive merit in polymer impregnation, leather processing, and fat liquoring (83).

The effect of temperature on the mechanical response of the polymer-leather composites remains to be treated. In Figure 20 are shown the torsional modulus-temperature curves for the three

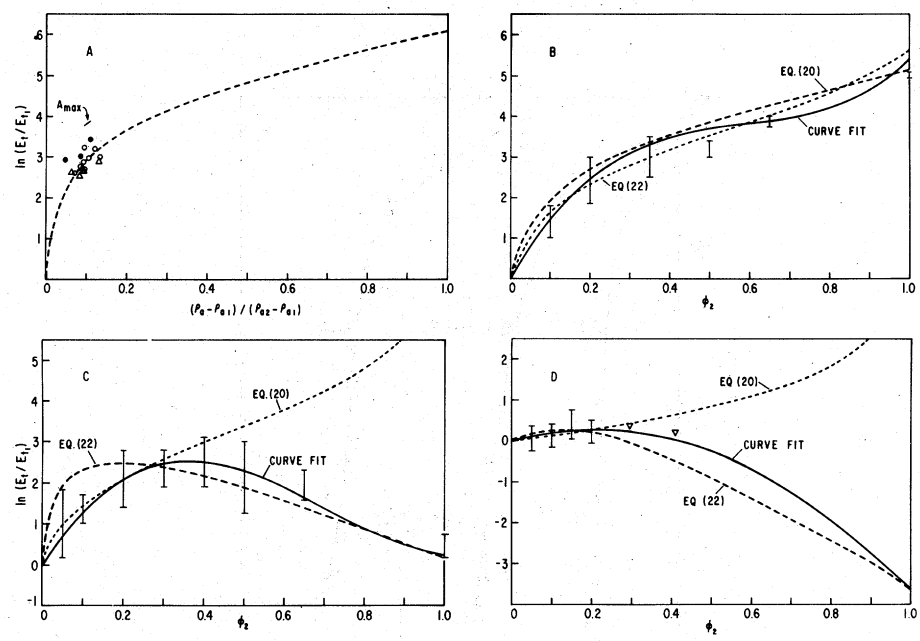

Fig. 19. The log of the torsional modulus ratio ln (E_t/E_{t1}) versus the fractional density increase $(\rho_a - \rho_{a1})/(\rho_{a2} - \rho_{a1})$ for all air-dried, untreated leather panels (Table VI) used with methanol extracted (circles) benzene extracted (triangles), and bulk-solution prepared composites (filled circles). The Halpin-Tsai equation (eq. (20)) was drawn for average values. Insert B (MMA), C (BA + MMA), and D (BA) compare curve fitted data (solid line) with eq. (20) (dotted line) and eq. (22) (dashed line).

neat modifying polymers of this work and the average values for the untreated leather controls (dashed line). Natural variability was again severe (bars). The shift in T_g, taken as the approximate inflection temperature, T_i - 5°C (4), for the modifying polymer is again apparent. The rapid rates of change of moduli for the neat modifying polymers contrasts with the rather featureless leather curve. This contrast was reduced (Fig. 21) for the composites. Curves for three polymer compositions, MMA (solid), BA + MMA, (dashed), and BA, (broken) are now closer to that of untreated leather (dotted curve). Gross phase separation was indicated for these composite materials because the T_g (downward arrows) of the parent polymer were essentially retained unchanged by the composites, and were little affected by composition (82c). This is in

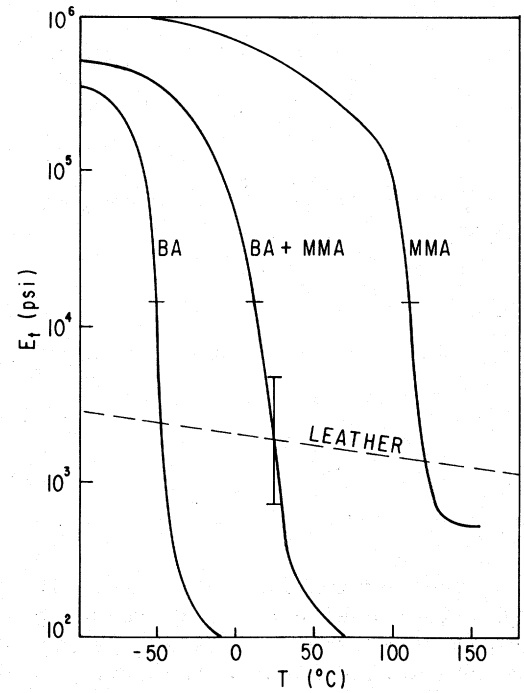

Fig. 20. Torsional modulus (E_{t2}) versus temperature curves for the base homo- and copolymers of this work (solid curves) and an average curve (E_{t1}) for methanol and benzene extracted leather controls. Slashes indicate the approximate inflection temperature, T_i at 14,500 psi (10^9 dynes cm^{-2}), with T_g estimated as T_i - 5°C. T_g was: MMA, 105°C; BA + MMA, 14°C; BA, -55°C. Bar denotes the extremes of variability of the leather apparent moduli at 23°C.

harmony with the morphologies illustrated in section C. However at low temperatures (T_i - 50°C) the torsional modulus of each composite system became dependent on polymer composition. The low temperature moduli increased as w_2 increased instead of reaching a common plateau of ~10^{10} dynes cm^{-2} characteristic of most polymer modified composite materials (82c). At high temperatures,

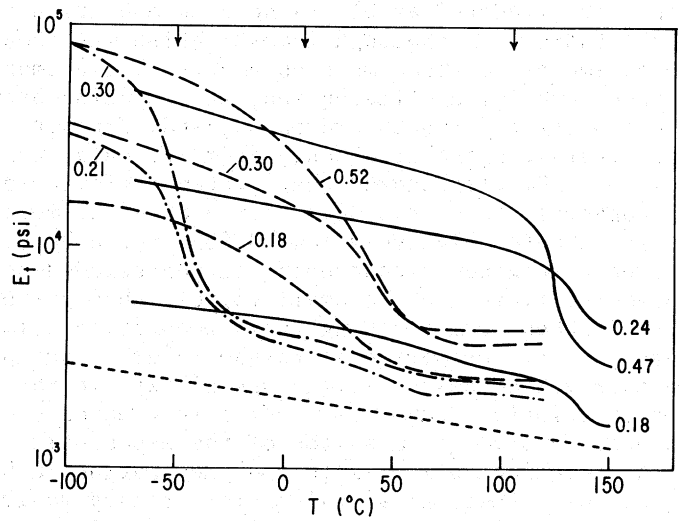

Fig. 21. Torsional modulus temperature curves for selections of composites for the three systems with varied composition, w_2. Solid lines represent data for MMA; dashed lines for BA + MMA; broken lines, BA. Comparative curves for the three systems are at similar w_2. Arrows indicate estimated T_g for the parent polymer from Figure 20. Dotted line is the average rate of change of the modulus for the controls, as in Figure 20.

T_i + 50°C, moduli of the starting leathers were approached. This shifting of moduli appears to result from the free space retained by each composition, as discussed in section A. This adds a porosity term (5e) to the moduli of each material. The fact that each phase was continuous, as seen in section C, and characterized by only weak interaction between phases further contributed to moduli residing between those of the starting materials. This permitted the mechanical response of the polymer-leather composites to shift from predominately plastic to predominately leather character as temperature rose.

SUMMARY AND CONCLUSIONS

Three acrylic monomers, MMA, BA + MMA, and BA were polymerized in the fibrous matrix of chrome-tanned 5 oz cattlehide by emulsion

polymerization with a persulfate-bisulfite redox initiating system and by AIBN initiated bulk or solution polymerization into acetone-dried samples. The widest feasible range of composition of the composites was studied. A thorough investigation was then undertaken of the parameters of the emulsion process, with emphasis on systems and feed deposition efficiencies, the relation between density and composition for both processes, and, finally, the determination of graft branch frequency from molecular weights of the bound polymer. Results showed that system efficiencies at 100% monomer conversion declined with increase in the molar volume of the monomer and were relatively low (0.635) for n-butyl acrylate. Likewise, increase in monomer concentration depressed deposition and bound polymer efficiencies to small values, thus preventing assumed graft branches from reaching their theoretical limit. Densities were directly proportional to the volume fraction of polymer when incremental space filling was allowed in the estimation of the bulk-solution composites. Kinetic studies of the emulsion process, involving comparison of the exponential intensity factors for the reaction variables for polymerization in both matrix and float with theoretical values for primary radical grafting and normal emulsion polymerization, indicated that little grafting was possible in these systems. Polymerization in the leather matrix appeared to be diffusion controlled throughout the lifetime of polymer deposition. Amplification of this conclusion negating grafting was obtained from decreased bound polymer found for finely divided leather dispersed in an extended float and by similar bound polymer deposits on simple impregnation of the leather with pre-formed polymer. Additional support was seen in the poor graft and deposition efficiencies. The coarse morphology, observed by light and scanning electron microscopy of composites and corresponding replicas of the continuous polymer phase, confirmed the improbability of the existance of many attachable sites on the collageneous fibers. Independence of the phases was confirmed by the observance of little protection of the matrix from bulk water absorption as a function of time and at final equilibrium. Mechanical properties revealed reduced relative tensile strengths (compared to those of untreated leather controls). Relative tensile and torsional moduli initially increased for composites having a small volume fraction, ϕ_2, of polymer (~0.20) for all systems regardless of the process and treatment used in their preparation. At higher ϕ_2 the viscoelastic properties of the modifying polymer dominated the composite properties. A modified theoretical equation, based on Halpin-Tsai parameters for fiber aggregation on air-dried controls, coupled with a term estimating empirically polymer-collagen fiber interaction, was successful in predicting the main trends of the relative moduli for all ϕ_2.

REFERENCES

1. E. F. Jordan, Jr., B. Artymyshyn, A. L. Everett, M. V. Hannigan, and S. H. Feairheller, J. Appl. Polym. Sci., 25, 2621 (1980).

2. E. F. Jordan, Jr. and S. H. Feairheller, J. Appl. Polym. Sci. 25, 2755 (1980).

3. E. F. Jordan, Jr., R. J. Carroll, M. V. Hannigan, B. Artymyshyn, and S. H. Feairheller, J. Appl. Polym.Sci. 26, 61 (1981).

4. E. F. Jordan, Jr., B. Artymyshyn, and S. H. Feairheller, J. Appl. Polym. Sci. 26, 463 (1981).

5. J. A. Manson and L. H. Sperling, Polymer Blends and Composites, Plenum Press, New York; 1976, a) pp. 77-119; b) pp. 121-168; c) pp. 237-270; d) 373-457; e) 363-369.

6. S. M. Atlas and H. Mark, Cellulose Chem. Technol., 3, 325 (1969).

7. J. C. Arthur, Adv. Macromol. Chem., W. M. Pasika, Ed., Academic Press, New York, 1970, Vol. 2, pp. 1-87.

8. M. S. Bains, J. Polym. Sci., C37, 125 (1972).

9. K. Arai, "Block and Graft Copolymerization," R. J. Ceresa, Ed., J. Wiley and Sons, New York, 1973, pp. 193-310.

10. W. J. Wosley, Ibid., pp. 311-333.

11. P. J. Nayak, J. Macromol. Sci., Revs. Macromol. Chem., C14, 193 (1976).

12. I. C. Watt, J. Macromol. Sci., Revs. Macromol. Chem., C5, 175 (1970).

13. R. Y. M. Huang and W. H. Rapson, J. Polym. Sci., C2, 169 (1963).

14. M. L. Rollins, A. M. Cannizzaro, F. A. Blouin, and J. C. Arthur, Jr., J. Appl. Polym. Sci., 12, 71 (1968).

15. R. Y. M. Huang, J. Appl. Polym. Sci., 10, 325 (1966).

16. V. S. Stannett, K. Araki, J. A. Gervasi, and S. W. McLeskey, J. Polym. Sci., A3, 3763 (1965).

17. A. H. Hebeish and P. C. Mehta, J. Appl. Polym. Sci., 12, 1265 (1968).

18. R. Y. M. Huang and P. Chandramouli, J. Appl. Polym. Sci., 12, 2549 (1968).

19. A. Kantouch, A. Hebeish, and A. Bendak, Europ. Polym. J., 1, 153 (1971).

20. M. Lipson and J. B. Speakman, J. Soc. Dyers & Colourists, 65, 390 (1949).

21. T. Valentine, J. Textile Inst., 46, T270 (1955).

22. B. K. Lohani, T. Valentine, and C. S. Whewell, J. Textile Inst., 49, T265 (1958).

23. M. Negishi, K. Arai, S. O. Kada, and J. Nagakura, J. Appl. Polym. Sci., 9, 3465 (1965).

24. A. Kantouch, S. Abdel-Fattah, and A. Hebeish, Polym. J. Japan, 3, 675 (1972).

25. A. Hebeish, M. H. El-Rafie, M. L. Khalel, and A. Bendak, J. Appl. Polym. Sci., 21, 1901 (1977).
26. A. Hebeish, A. Bendak, and A. Kantouch, J. Appl. Polym. Sci., 15, 2733 (1971).
27. A. Bendak, M. L. Khalil, M. H. El-Rafie, and A. Hebeish, J. Appl. Polym. Sci., 19, 335 (1975).
28. A. Bendak and A. Hebeish, J. Appl. Polym. Sci., 17, 1953 (1973).
29. R. Y. M. Huang and P. Chandramouli, J. Polym. Sci. A1, 7, 1393 (1969).
30. R. Y. M. Huang, B. Immergut, E. H. Immergut, and W. H. Rapson, J. Polym. Sci., A1, 1257 (1963).
31. K. Arai, Polymer, 18, 211 (1977).
32. G. Mino and S. Kaizerman, J. Polym. Sci., 31, 242 (1958).
33. J. L. Williams, D. K. Woods, V. S. Stannett, S. B. Sello, and C. V. Stevens, Int. J. Appl. Radiation and Isotopes, 26, 159 (1975).
34. J. L. Williams and V. Stannett, Textiles Res. J., 38, 1065 (1968).
35. Y. Ikada, Adv. Polym. Sci., 29, 47 (1978).
36. R. W. Lenz, Organic Chemistry of Synthetic High Polymers, Interscience, New York, 1967; a) pp. 364-365; b) pp. 711-713.
37. Y. Ogiwara, Y. Ogiwara, and H. Kubata, J. Polym. Sci., A16, 1489 (1968).
38. A. H. Korn, S. H. Feairheller, and E. M. Filachione, J. Am. Leather Chem. Assoc., 67, 111 (1972).
39. A. H. Korn, M. M. Taylor, and S. H. Feairheller, J. Am. Leather Chem. Assoc., 68, 224 (1973).
40. E. H. Harris, M. M. Taylor, and S. H. Feairheller, J. Am. Leather Chem. Assoc., 69, 182 (1974).
41. G. Mino, S. Kaizerman, and E. Rasmussen, J. Polym. Sci., 39, 523 (1959).
42. R. A. Wallace and D. G. Young, J. Polymer Sci. A1, 4, 1179 (1966).
43. G. Mino, S. Kaizerman, and E. Rasmussen, J. Polym. Sci., 38, 393 (1959).
44. A. A. Katai, V. K. Kulshiestha, and R. W. Marchessoult, J. Polym. Sci. C, 2, 403 (1963).
45. A. Rout, S. P. Rout, B. C. Singh, and M. Santappa, Macromol. Chem., 178, 639 (1977).
46. L. A. Gugliemelli, C. J. Swanson, and W. A. Doone, J. Polym. Sci., Polym. Chem. Ed., 11, 2451 (1973).
47. W. V. Smith and R. H. Ewart, J. Chem. Physics, 16, 592 (1948).
48. W. V. Smith, J. Am. Chem. Soc., 70, 3695 (1948).
49. J. L. Gardon, J. Polym. Sci. A-1, 6, 623 (1968).
50. J. L. Gardon, J. Polym. Sci. A-1, 6, 665 (1968).
51. R. M. Fitch, M. B. Prenosil, and K. J. Sprich, J. Polym. Sci., C27, 95 (1969).

52. R. M. Fitch and C. H. Tsai, in Polymer Colloids, R. M. Fitch, Ed., Plenum Press, New York, 1971, pp. 73-102.
53. M. M. Taylor, E. H. Harris, and S. H. Feairheller, J. Am. Leather Chem. Assoc., 72, 294 (1977).
54. T. Landells and C. S. Whewells, J. Soc. Dyers and Colourists, 71, 171 (1955).
55. T. Valentine, J. Textile Inst., 47, T1 (1956).
56. W. M. Kaeppner and R. Y. M. Huang, Textile Res. J., 35, 504 (1965).
57. F. A. Blouin and J. C. Arthur, Jr., Textile Res. J., 33, 727 (1963).
58. J. C. Arthur, Jr., and F. A. Blouin, J. Appl. Polym. Sci., 8, 2813 (1964).
59. J. L. Williams, V. S. Stannett, L. G. Roldan, S. B. Sello, and C. V. Stevens, Int. J. Appl. Radiation and Isotopes, 26, 169 (1975).
60. F. A. Blouin, N. J. Morris, and J. C. Arthur, Jr., Textile Res. J., 36, 309 (1966).
61. R. J. Demint, J. C. Arthur, Jr., A. R. Markezich, and W. F. McSherry, Textile Res. J., 32, 918 (1962).
62. M. W. Andrews, R. L. D'Arcey, and I. C. Watt, J. Polym. Sci., Polym. Letters, 3, 441 (1965).
63. W. R. Goynes and J. A. Harris, J. Polym. Sci., C37, 277 (1972).
64. J. A. Swift, Chemistry of Natural Protein Fibers, A. S. Osquith, Ed., Plenum Press, New York, 1977, pp. 81-146.
65. K. P. Rao, K. T. Joseph, and Y. Nayudamma, J. Appl. Polym. Sci., 16, 975 (1972).
66. J. C. Arthur, Jr. and R. J. Demint, Textile Res. J., 30, 505 (1960).
67. F. A. Blouin, N. J. Morris, and J. C. Arthur, Jr., Textile Res. J., 38, 710 (1968).
68. F. A. Blouin, A. M. Cannizzaro, J. C. Arthur, Jr., and M. L. Rollins, Textile Res. J., 38, 811 (1968).
69. F. L. Saunders and R. C. Sovish, J. Appl. Polym. Sci., 7, 357 (1963).
70. T. Mares and J. C. Arthur, Jr., J. Polym. Sci., C37, 349 (1972).
71. I. C. Watt, J. Macromol. Sci. Chem., A4, 1079 (1970).
72. H. L. Needles, Textile Res. J., 48, 506 (1978).
73. D. S. Varma and R. K. Sarkar, Die Angewandte Makromolekulare Chemie, 37, 177 (1974).
74. L. J. Wolfram and J. Menkert, Am. Dyestuff Reptr., 56, 110 (1967).
75. J. R. Kanagy, Chemistry and Technology of Leather, Vol. 4, F. O'Flaherty, W. T. Roddy, and R. M. Lollar, Eds., Reinhold Publishing Corp., New York, 1965, pp. 369-416.
76. I. V. Yannas, J. Macromol. Sci., Revs. Macromol. Chem., C7, 49 (1972).

77. J. R. Kanagy, E. B. Randall, T. J. Carter, R. A. Kinmouth, and C. W. Mann, J. Am. Leather Chem. Assoc., 47, 726 (1952).

78. R. M. Lollar, J. Am. Leather Chem. Assoc., 54, 306 (1959).

79. J. R. Kanagy, J. Am. Leather Chem. Assoc., 50, 112 (1955).

80. K. P. Rao, K. T. Joseph, and Y. Nayudamma, Leather Sci., 19, 27 (1972).

81. K. P. Rao, D. H. Kamat, K. T. Joseph, M. Santappa, and Y. Nayudamma, Leather Sci., 21, 111 (1974).

82. L. E. Nielsen, Mechanical Properties of Polymers and Composites, Parts I and II, Marcel Dekker Inc., New York, 1974; a) pp. 379-452; b) pp. 453-510; c) pp. 208-215.

83. T. C. Thorstensen, Practical Leather Technology, R. E. Krieger Publishing Corp., New York, 1976, pp. 190-207.